

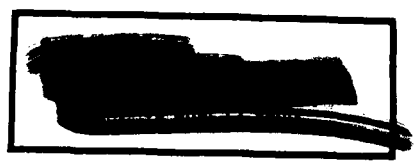
~~TOP SECRET~~

Declassified by authority of NASA  
Classification Change Notices No. 113  
Dated \*\* 6/23/67

EFFECT OF WING PIVOT LOCATION ON LONGITUDINAL AERODYNAMIC  
CHARACTERISTICS OF A VARIABLE-SWEEP WING  
HAVING AN M PLANFORM

By William P. Henderson and Edward J. Ray

Langley Research Center  
Langley Station, Hampton, Va.



~~CLASSIFIED DOCUMENT-TITLE UNCLASSIFIED  
This document contains information affecting the  
national defense of the United States within the  
meaning of the Espionage Laws, Title 18, U.S.C.,  
Secs. 793 and 794, the transmission or revelation  
of information in any manner to an unauthorized person  
is prohibited by law.~~

NOTICE  
This document should not be returned after it has  
satisfied your requirements. It may be disposed  
of in accordance with your local security regula-  
tions or the appropriate provisions of the Industrial  
Security Manual for Safe-Guarding Classified  
Information.

NATIONAL AERONAUTICS AND SPACE ADMINISTRATION



REF ID: A60110

EFFECT OF WING PIVOT LOCATION ON LONGITUDINAL AERODYNAMIC

CHARACTERISTICS OF A VARIABLE-SWEEP WING

HAVING AN M PLANFORM\*

By William P. Henderson and Edward J. Ray  
Langley Research Center

SUMMARY

17228

An investigation was made in the Langley high-speed 7- by 10-foot tunnel to determine the effect of wing pivot location on the longitudinal aerodynamic characteristics of a variable-sweep wing having an M planform. The investigation was made with and without horizontal tails and with and without engine packs. The effects of wing leading-edge chord extension are also included. Investigations were made at a Mach number of 0.40, at angles of attack from  $-3^{\circ}$  to  $22^{\circ}$ , and for a Reynolds number per foot of  $2.52 \times 10^6$ .

The results indicate that moving the pivot outboard causes the unstable break in the pitching-moment variation with lift coefficient to occur at lower values of lift coefficient and generally to be more severe. However, the more outboard the pivot location, the more favorable is the variation in the longitudinal stability level with wing sweep.

The variation of the longitudinal stability parameter with wing leading-edge sweep angle was accurately predicted by discrete vortex theory. However, the lift-curve slope was slightly higher than estimated for all wing-sweep positions and pivot locations. *Conf*

*Butler*

INTRODUCTION

The National Aeronautics and Space Administration has investigated a number of configurations in the study of the longitudinal stability characteristics of variable-sweep wings. Examples of some of these various configurations are presented in references 1 to 3. Two major problems associated with variable-sweep wings are the variations of aerodynamic center with wing-sweep angle and the variation of pitching moment with lift coefficient. As reported in reference 4 the variation in aerodynamic center with wing sweep for arrow-type wings can be controlled by the location of the wing pivot point. It was also shown in reference 4 that for arrow-type wings a pivot location that minimizes the aerodynamic-center variation is generally accompanied by variation of pitching

\*Title, Unclassified.

*[Redacted]*

moment with lift coefficient that becomes less stable above moderate lift coefficients because of the high upwash angularities induced on the outer wing panel by the inboard fixed wing panel. For configurations on which the horizontal tails can be located in a low position relative to the wing-chord plane the longitudinal stability decrease at moderate lift coefficients can be eliminated. For configurations on which, for practical reasons such as engine efflux effects, the tail cannot be located below the wing-chord plane, other means must be found for eliminating or decreasing the longitudinal instability. Previous investigations (refs. 5 and 6) have indicated that the pitch-up problem associated with arrow wings can be minimized by the use of M planform wings. In an attempt to combine the desirable characteristics of the variable-sweep concept with the desirable pitch characteristics of the M planforms, an investigation was conducted on three series of wings simulating variable-sweep M planforms with various pivot locations. Therefore, the purpose of this paper is to present the longitudinal stability characteristics of these series of M planform wings which incorporate variable-sweep outboard panels.

In each of these series the wing in the highly sweptback position was identical. Each series of wings employed a different simulated wing pivot location which resulted in different wing planforms at the lower wing-sweep angles. The wing pivots were located at 60, 45, and 30 percent of the sweptback wing semi-span. Wing-sweep angles of 15°, 30°, and 72° were investigated for each pivot location. Inasmuch as the investigation was primarily concerned with the longitudinal stability trends, these wings employed flat-plate airfoil sections with rounded leading edges and blunt trailing edges to minimize model fabrication time.

The investigation was made with and without horizontal tails on the configurations. The effect of wing leading-edge chord extensions and engine packs is also included. Estimates, computed by using discrete vortex theory, of the variation of the lift-curve slope and the longitudinal stability parameter with wing leading-edge sweep angle were made for these three series of wings. A comparison of these computations with experiment is presented herein. This investigation was conducted in the Langley high-speed 7- by 10-foot tunnel at a Mach number of 0.40 and for a Reynolds number per foot of  $2.52 \times 10^6$ . The angle-of-attack range varied from -3° to 22°.

COEFFICIENTS AND SYMBOLS

The forces and moments measured on this configuration are presented about the wind axis system. All coefficients are nondimensionalized with respect to the geometric characteristics associated with the maximum sweep position of 72°. The moment reference points for each wing pivot location are shown in figure 1.

- b wing span, ft
- $C_D$  drag coefficient,  $\frac{\text{Drag}}{qS}$

- $C_L$  lift coefficient,  $\frac{\text{Lift}}{qS}$
- $C_{L\alpha}$  lift-curve slope measured between  $\pm 1^\circ$  angle of attack, per deg
- $\frac{C_{lc}}{C_{Lcav}}$  nondimensional span-loading coefficient
- $C_m$  pitching-moment coefficient,  $\frac{\text{Pitching moment}}{qS\bar{c}}$
- $C_{mC_L}$  longitudinal stability parameter measured between  $\pm 0.1$  lift coefficient
- $\bar{c}$  mean aerodynamic chord, 1.133 ft
- $c_{av}$  average wing chord, ft
- $q$  dynamic pressure, lb/sq ft
- $S$  wing reference area, 1.727 sq ft
- $y'$  distance to simulated wing pivot from plane-of-symmetry line, ft
- $y$  distance measured along wing span from plane-of-symmetry line, ft
- $\alpha$  angle of attack, deg
- $\Lambda_{LE}$  leading-edge sweep angle of the movable panel, deg

### MODELS

Seven wings of 3/16-inch flat plates and representing various leading-edge sweep angles and wing pivot locations were constructed and arranged in three series as shown in figures 1(a), 1(b), and 1(c). The  $72^\circ$  sweptback wing was the same for each series. This highly sweptback wing had an M planform, with the leading-edge break located at 33 percent of the wing semispan. A different pivot location was simulated by each series of wings.

These simulated pivots were located at 60, 45, and 30 percent of the wing semispan and at 60 percent of the streamwise chord of the sweptback wing as shown in figures 1(a), 1(b), and 1(c), respectively. These wings were 3/16-inch flat plates with rounded leading edges and blunt trailing edges. No attempt was made to fair the wings into the fuselage and therefore the drag characteristics should be used with caution.



The horizontal tails were 1/8-inch flat plates with rounded leading edges and blunt trailing edges and were capable of being mounted on the vertical tails in two positions as shown in figure 1(b).

The engine packs utilized on this configuration simulated packs housing two engines each and were mounted beneath the wing as shown in figure 1(c). A drawing of the engine packs is shown in figure 1(d).

The wing leading-edge chord extension utilized on one of these configurations extended from  $\frac{y}{b/2} = 0.65$  to  $\frac{y}{b/2} = 0.92$  (fig. 1(b)) and had a chord equal to 30 percent of the local wing chord. This chord extension was deflected down  $30^\circ$  with respect to the wing-chord plane.

### TESTS AND CORRECTIONS

The investigation was made in the Langley high-speed 7- by 10-foot tunnel at a Mach number of 0.40 which corresponds to a dynamic pressure of about 213 pounds per square foot and a Reynolds number per foot of  $2.52 \times 10^6$ .

Lift, drag, and pitching moment were measured through an angle-of-attack range of  $-3^\circ$  to  $22^\circ$ . The angle of attack was corrected for deflection of the sting support system under load. The drag data have been corrected neither for the effects of base pressure acting on the fuselage and nacelles nor for the internal drag of the nacelles. These tests were made without artificial transition strips on the model. The jet-boundary and blockage corrections are negligible for the open-slot configuration of the tunnel.

The moment reference point (shown in fig. 1) was chosen such that the  $15^\circ$  sweptback wing for each pivot location was stable at  $0.05\bar{c}$  with the horizontal tails off.

### PRESENTATION OF DATA

The data are presented in the following figures:

	Figure
Effect of wing leading-edge sweep angle on longitudinal aerodynamic characteristics of configuration with horizontal tails and engine packs off.	
$\left(\frac{y'}{b/2}\right)_{\Lambda_{LE}=72^\circ} = 0.60$ . . . . .	2
$\left(\frac{y'}{b/2}\right)_{\Lambda_{LE}=72^\circ} = 0.45$ . . . . .	3



$$\left(\frac{y'}{b/2}\right)_{\Lambda_{LE}=72^\circ} = 0.30 \dots \dots \dots 4$$

Effect of pivot location on variation of longitudinal stability parameter with wing leading-edge sweep angle for configuration with horizontal tails and engine packs off . . . . . 5

Effect of pivot location on pitching-moment variation with lift coefficient for configuration with horizontal tails and engine packs off. (Transferred to same stability level through zero lift coefficient.) . . . . . 6

Effect of wing leading-edge sweep angle on longitudinal aerodynamic characteristics of configuration with horizontal tails on (high location) and engine packs off.

$$\left(\frac{y'}{b/2}\right)_{\Lambda_{LE}=72^\circ} = 0.45 \dots \dots \dots 7$$

$$\left(\frac{y'}{b/2}\right)_{\Lambda_{LE}=72^\circ} = 0.30 \dots \dots \dots 8$$

Effect of location of horizontal tails on longitudinal aerodynamic characteristics of configuration with 15° of leading-edge sweep with engine packs off.

$$\left(\frac{y'}{b/2}\right)_{\Lambda_{LE}=72^\circ} = 0.45 \dots \dots \dots 9$$

Effect of wing leading-edge sweep angle on longitudinal aerodynamic characteristics of configuration with horizontal tails (high location) and engine packs on.

$$\left(\frac{y'}{b/2}\right)_{\Lambda_{LE}=72^\circ} = 0.30 \dots \dots \dots 10$$

Effect of chord extension on longitudinal aerodynamic characteristics of configuration with 15° of leading-edge sweep and horizontal tails on (high location) and engine packs off.

$$\left(\frac{y'}{b/2}\right)_{\Lambda_{LE}=72^\circ} = 0.45 \dots \dots \dots 11$$



Comparison of experimental and computed variation of lift-curve slope and longitudinal stability parameter with wing leading-edge sweep angle of configuration with horizontal tails and engine packs off.

(y') / (b/2) at Lambda\_LE = 72 degrees = 0.60 . . . . . 12

(y') / (b/2) at Lambda\_LE = 72 degrees = 0.45 . . . . . 13

(y') / (b/2) at Lambda\_LE = 72 degrees = 0.30 . . . . . 14

Computed span-load distribution for the wing alone, at various wing leading-edge sweep angles.

(y') / (b/2) at Lambda\_LE = 72 degrees = 0.60 . . . . . 15

(y') / (b/2) at Lambda\_LE = 72 degrees = 0.45 . . . . . 16

(y') / (b/2) at Lambda\_LE = 72 degrees = 0.30 . . . . . 17

RESULTS AND DISCUSSION

The longitudinal aerodynamic characteristics for the wing-body combinations are presented in figures 2 to 4 for the three pivot locations investigated. These data indicate decreases in the level of longitudinal stability for all sweep angles for moderate angles of attack and lift coefficients. The degree of the stability decrease with lift coefficient is dependent on both simulated pivot location and level of longitudinal stability at zero lift coefficient. It is to be noted that the moment references used in the data of figures 2 to 4 which varied for the different pivot locations were chosen so that the low-sweep wings (Lambda\_LE = 15 degrees) were stable at 0.05c.

In order to illustrate separately the effect of simulated pivot location on the variation of longitudinal stability level with wing-sweep angle, and the pitching-moment variation with lift coefficient, figures 5 and 6 have been prepared. As seen in figure 5, where the low-sweep wings (Lambda\_LE = 15 degrees) have been adjusted to the same stability level, the more outboard the pivot location, the more favorable is the variation in longitudinal stability level with wing sweep. However, with regard to the variation of pitching moment with lift coefficient, figure 6 (data adjusted to a common stability level) indicates that moving the



simulated pivot location outboard causes the unstable break in the pitching-moment curve to occur at lower values of lift coefficient and generally to be more severe. The effect of pivot location on the aerodynamic-center variation with sweep angle and the pitching-moment variation with lift coefficient for the present M planform wings are therefore similar to the arrow-wing characteristics of reference 4.

The effect of the horizontal tail on the longitudinal aerodynamic characteristics of the configuration with the pivot located at 45 percent and 30 percent of the sweptback wing semispan can be seen by comparing figure 3 with figure 7 and figure 4 with figure 8. These data indicate that the addition of the horizontal tails in the high location had no appreciable effect on the lift coefficient at which instability occurs or on the instability level above this lift coefficient. Little or no improvement in these characteristics results from lowering the tails to the midhigh position as shown by figure 9. However, for this configuration the horizontal tails could be placed in a lower position than the positions investigated without experiencing jet-efflux effects. If these tails had been placed in a lower position, beneficial effects on the pitching-moment variation with lift coefficient could possibly have been obtained, as indicated by the data of reference 7. These data presented in this reference were obtained during a tail-height investigation on a configuration incorporating a variable-sweep arrow wing. The fuselage of the present investigation was not designed to incorporate horizontal tails in positions lower than those investigated.

The effect of the engine packs on the longitudinal stability characteristics for the configuration with the pivot located at 30 percent of the sweptback wing semispan can be seen by comparing figure 8 with figure 10. These data show that the addition of the engine packs produced a positive increment in the pitching moment at zero lift with essentially no change in the variation of pitching moment with lift coefficient.

The addition of a chord extension of about 30 percent of the local wing chord to the 15° sweptback wing at  $\frac{y}{b/2} = 0.65$  to  $\frac{y}{b/2} = 0.92$  increased the lift coefficient at which pitch-up occurred from about 0.40 to 0.80. (See fig. 11.)

A comparison of the experimental and computed variations of longitudinal stability parameters with wing leading-edge sweep angle (computed by discrete vortex theory as presented in ref. 8) is shown for the three pivot locations in figures 12 to 14. The computed longitudinal stability has been adjusted to 0.05c for the wing with 15° of leading-edge sweep. These data show that the variation of longitudinal stability parameter  $C_{mC_L}$  with wing leading-edge sweep angle is accurately predicted by this method.

A comparison of the experimental and computed variation of lift-curve slope with wing leading-edge sweep angle is also shown on these figures. These data indicate that the method of reference 8, which is for a wing alone, slightly underestimates the lift-curve slope for all pivot locations and wing-sweep positions. This slight difference between the computed and experimental values is



CONFIDENTIAL

presumed attributable to body induction effects on the wing, for which this method of computation does not account.

Inasmuch as the span-load distribution is useful in structural analysis, the span-load distributions from which the lift-curve slopes and the longitudinal stability parameters were obtained are included to allow for structural or load analysis. The span-load distributions which were computed by the method of reference 8 are presented for wing leading-edge sweep angles of  $15^\circ$ ,  $30^\circ$ ,  $50^\circ$ , and  $72^\circ$  for pivot locations of 60 and 45 percent of the sweptback wing semi-span in figures 15 and 16, and for wing leading-edge sweep angles of  $15^\circ$ ,  $30^\circ$ , and  $72^\circ$  for the pivot located at 30 percent of the sweptback wing semispan in figure 17.

### CONCLUSIONS

An investigation to determine the effect of pivot location on the longitudinal aerodynamics of a variable-sweep wing having an M planform indicated the following results:

1. Moving the pivot location outboard caused the unstable break in the pitching-moment variation with lift coefficient to occur at lower values of lift coefficient and generally to be more severe. However, the more outboard the pivot location, the more favorable was the variation in longitudinal stability level with wing sweep.
2. The variations of longitudinal stability with wing leading-edge sweep angle were accurately predicted by discrete vortex theory. However, the experimental lift-curve slope was slightly higher than estimated for all wing-sweep positions and pivot locations.

Langley Research Center,  
National Aeronautics and Space Administration,  
Langley Station, Hampton, Va., June 25, 1964.

CONFIDENTIAL



## REFERENCES

1. Vogler, Raymond D., and Turner, Thomas R.: Exploratory Low-Speed Wind-Tunnel Stability Investigation of a Supersonic Transport Configuration With Variable-Sweep Wings. NASA TM X-597, 1961.
2. Henderson, William P.: Low-Speed Longitudinal Stability Characteristics of a Supersonic Transport Configuration With Variable-Sweep Wings Employing a Double Inboard Pivot. NASA TM X-744, 1962.
3. Alford, William J., Jr., Hammond, Alexander D., and Henderson, William P.: Low-Speed Stability Characteristics of a Supersonic Transport Model With a Blended Wing-Body, Variable-Sweep Auxiliary Wing Panels, Outboard Tail Surfaces, and Simplified High-Lift Devices. NASA TM X-802, 1963.
4. Baals, Donald D., and Polhamus, Edward C.: Variable Sweep Aircraft. *Astronautics and Aerospace Eng.*, vol. 1, no. 5, June 1963, pp. 12-19.
5. Fournier, Paul G.: Effects of Spanwise Location of Sweep Discontinuity on the Low-Speed Longitudinal Stability Characteristics of a Complete Model With Wings of M and W Plan Form. NACA RM L54K23, 1955.
6. Henderson, William P.: Longitudinal Stability Characteristics of Low-Aspect-Ratio Wings Having Variations in Leading- and Trailing-Edge Contours. NASA TN D-1796, 1964.
7. Lockwood, Vernard E., McKinney, Linwood W., and Lamar, John E.: Low-Speed Aerodynamic Characteristics of a Supersonic Transport Model With a High-Aspect-Ratio Variable-Sweep Warped Wing. NASA TM X-979, 1964.
8. Campbell, George S.: A Finite-Step Method for the Calculation of Span Loadings of Unusual Plan Forms. NACA RM L50L13, 1951.

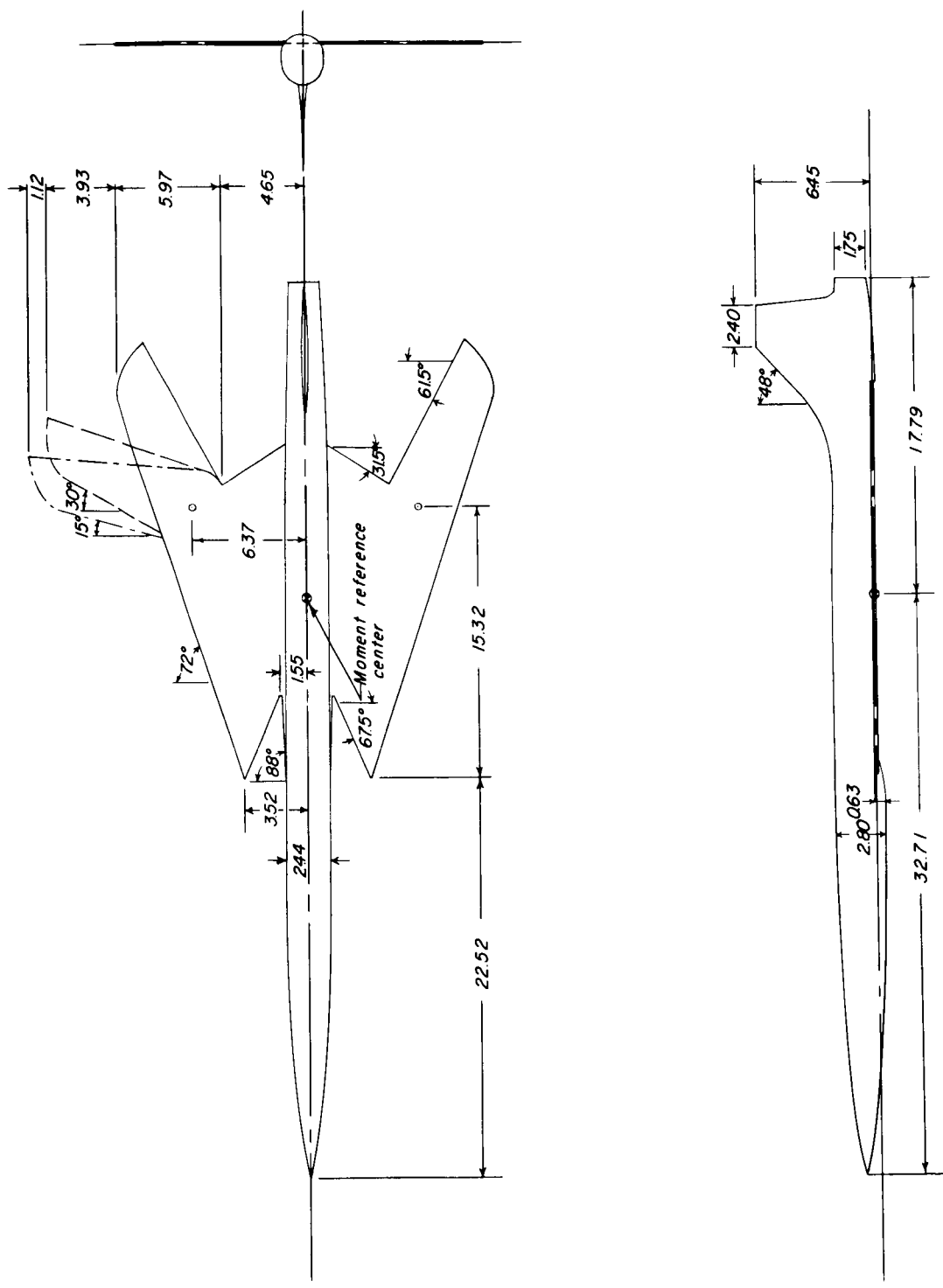
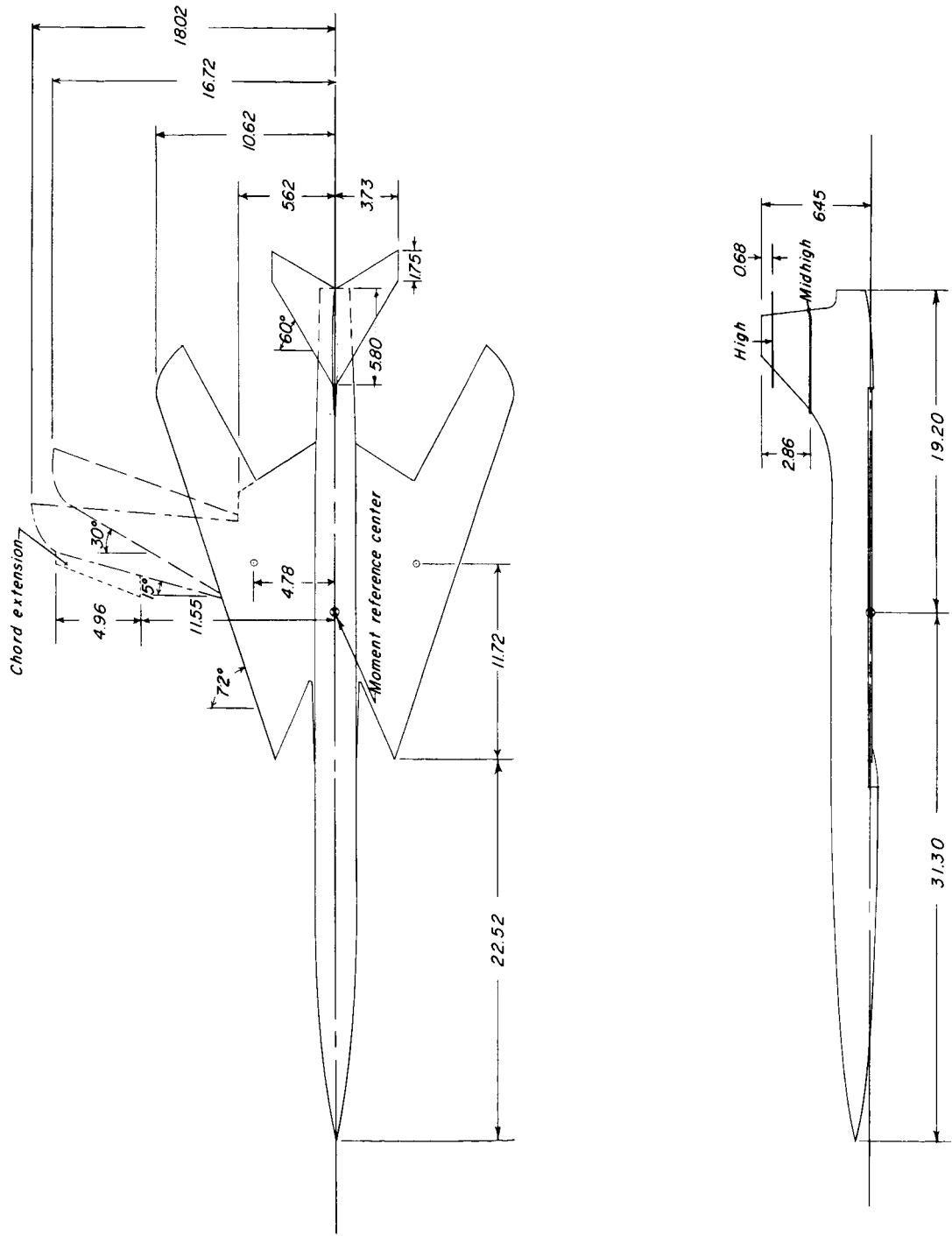
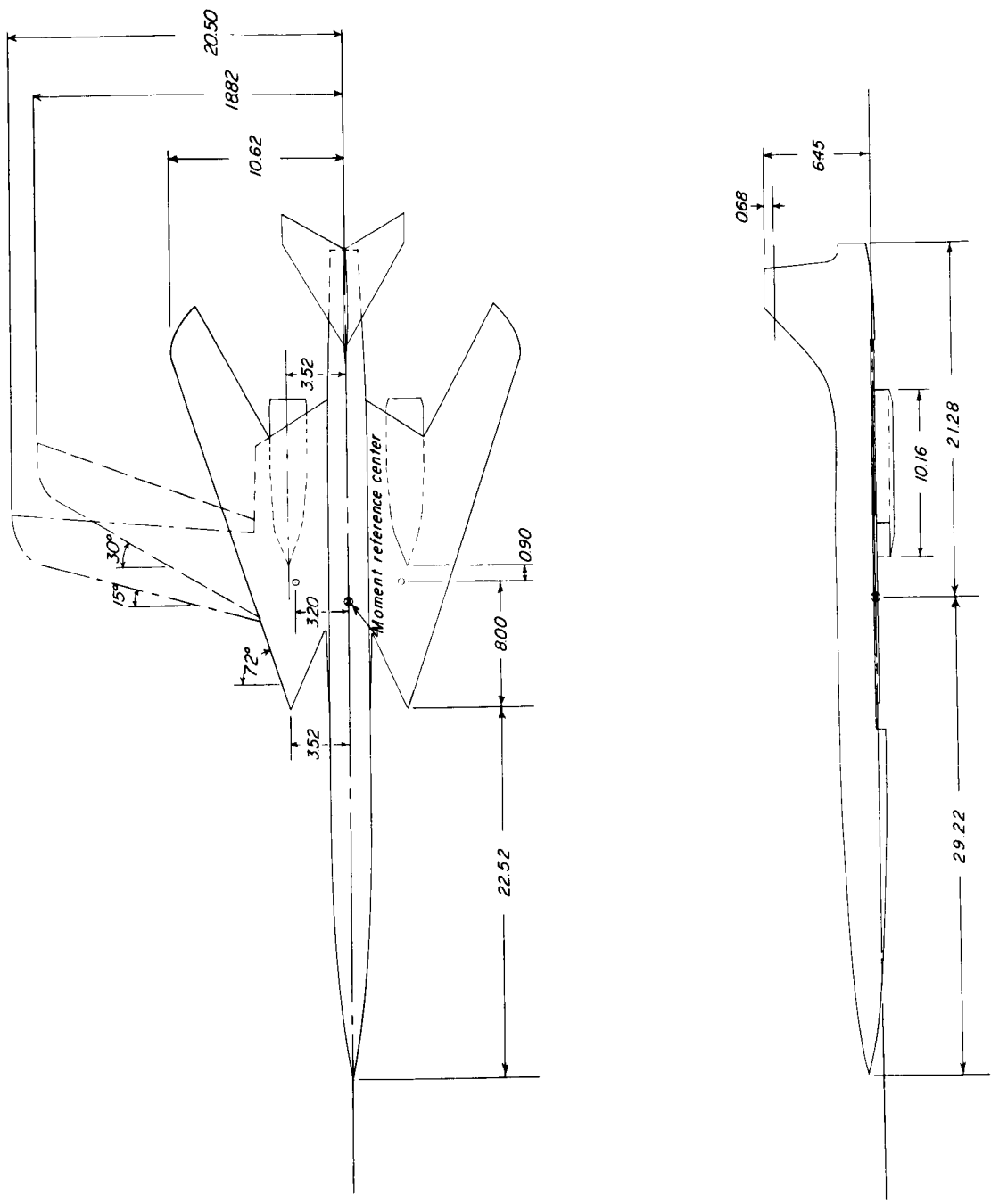


Figure 1.- Drawing of configurations investigated. (All dimensions are in inches unless otherwise noted.)



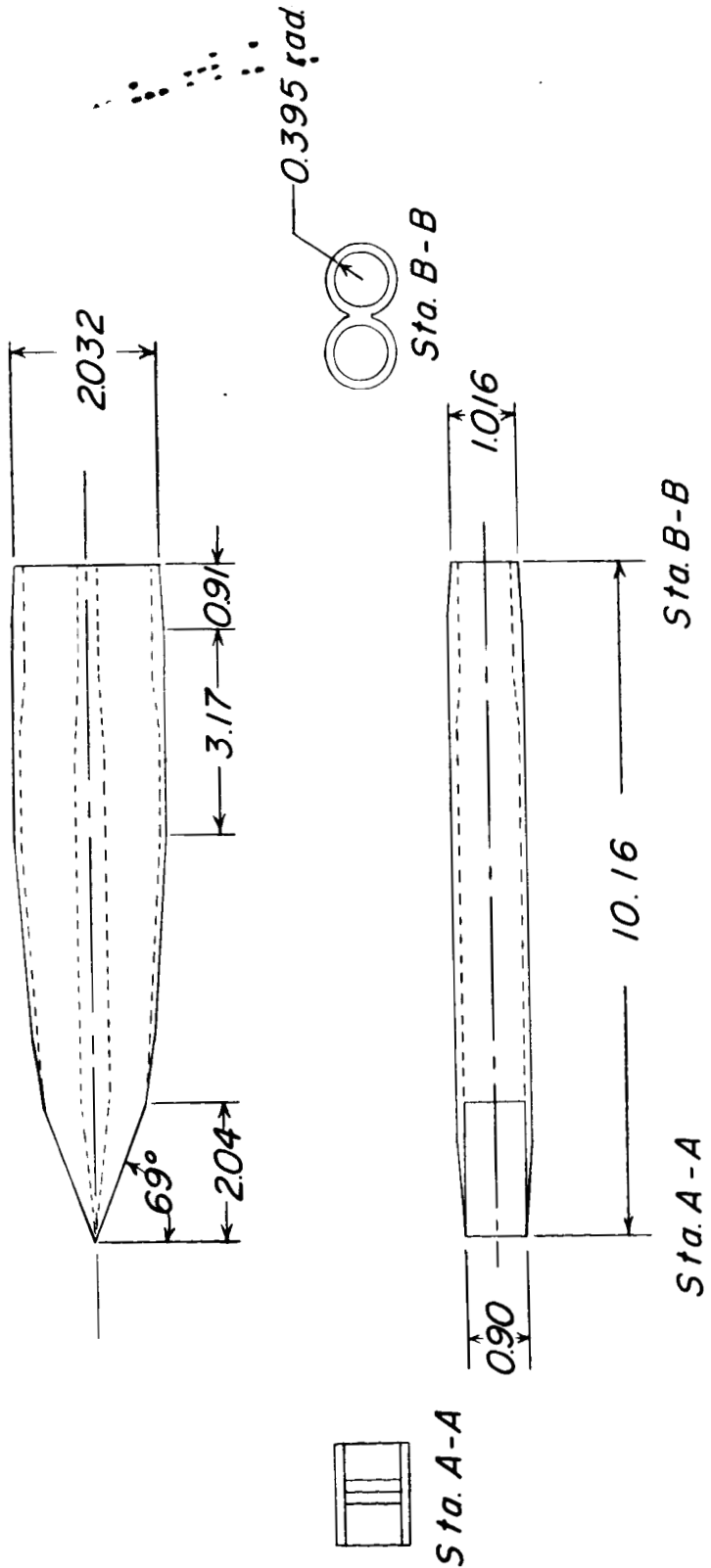
(b)  $\frac{y'}{b/2} = 0.45$ .

Figure 1.- Continued.



(c)  $\frac{y'}{b/2} = 0.30.$

Figure 1.- Continued.



(d) Drawing of engine packs.

Figure 1.- Concluded.

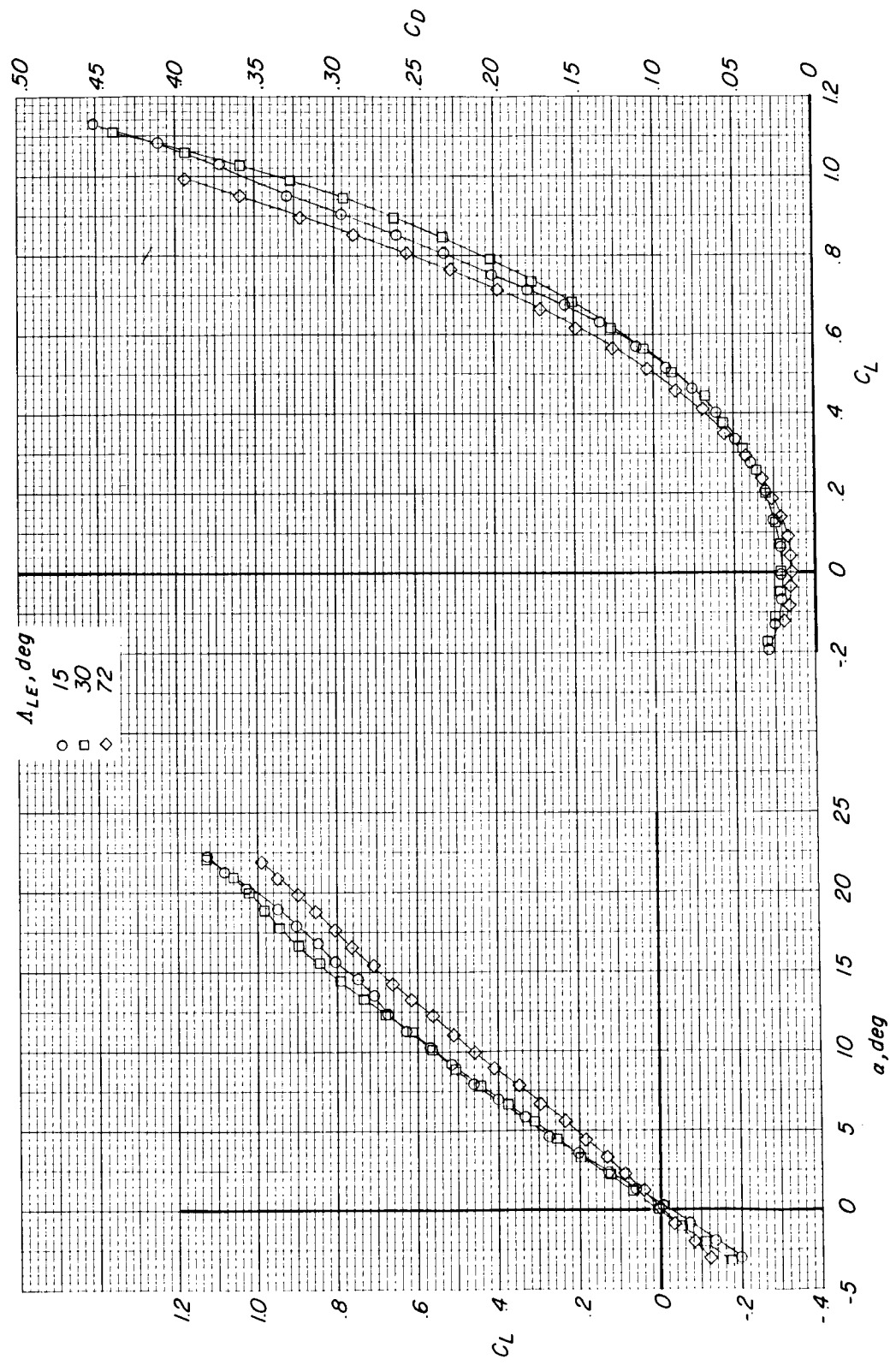


Figure 2.- Effect of wing leading-edge sweep angle on longitudinal aerodynamic characteristics of configuration with horizontal tails and engine packs off.  $\left(\frac{y'}{b/2}\right)_{\alpha_{LE}=72^\circ} = 0.60$ .

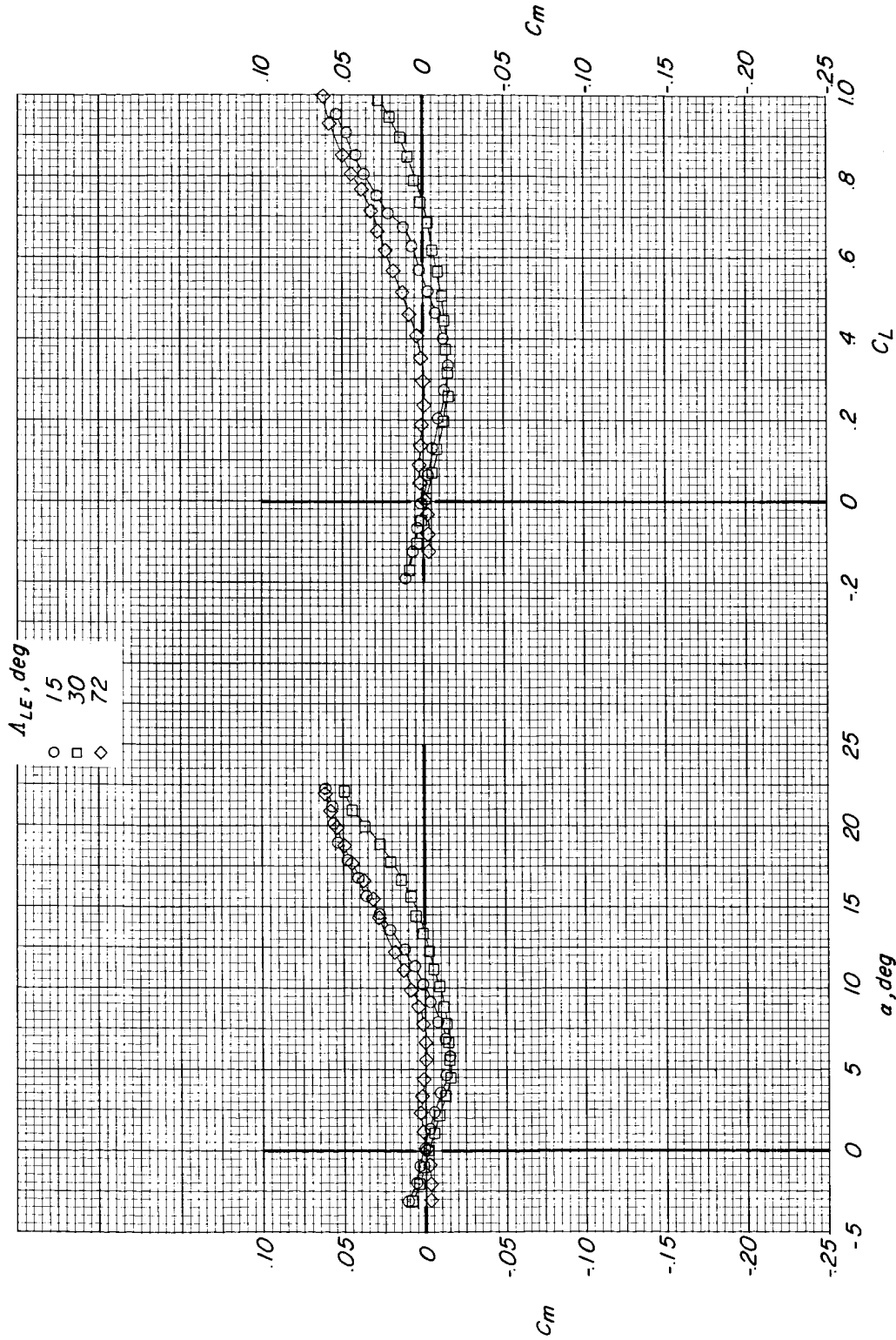


Figure 2.- Concluded.



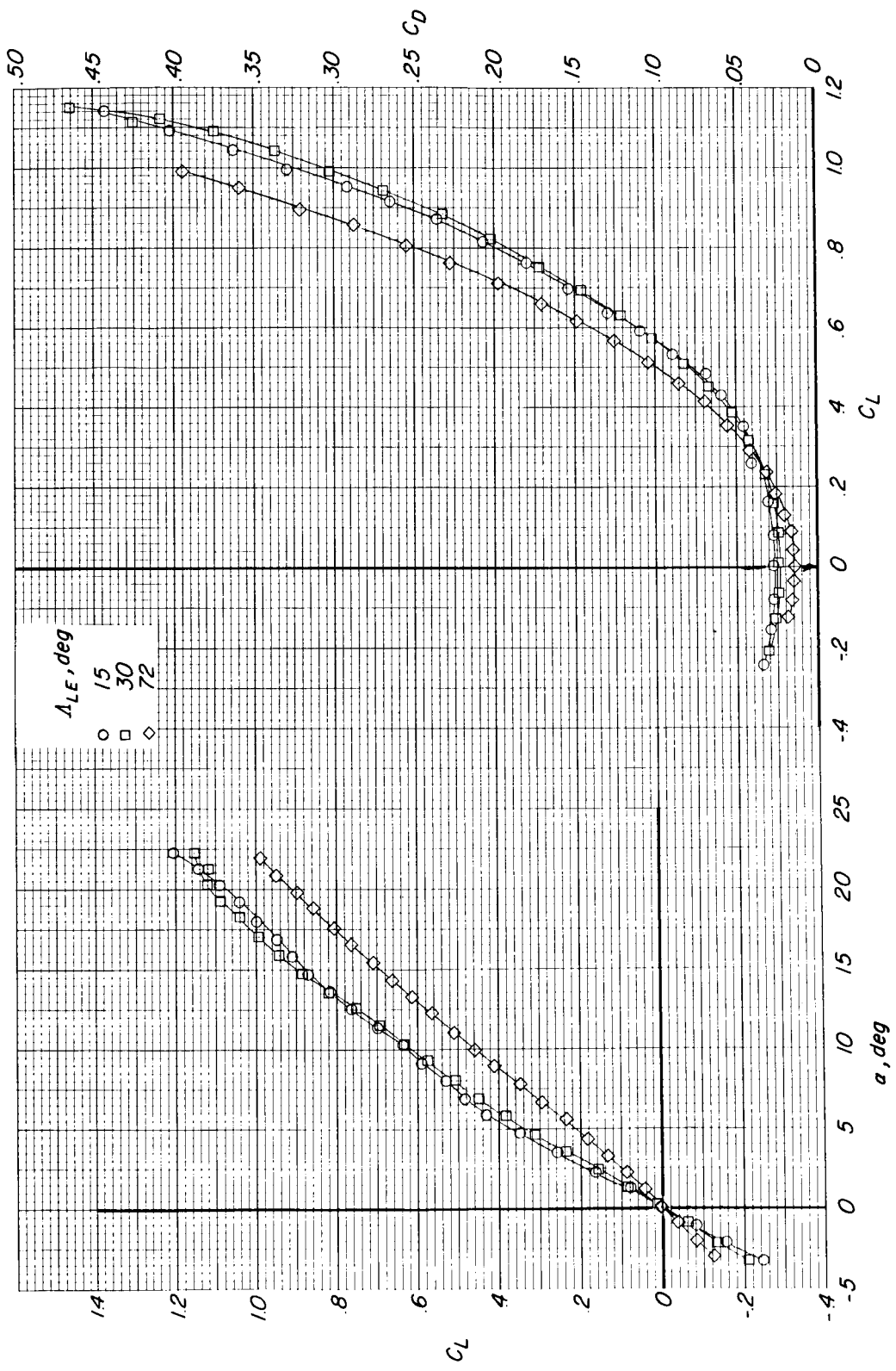


Figure 3.- Effect of wing leading-edge sweep angle on longitudinal aerodynamic characteristics of configuration with horizontal tails and engine packs off.  $\left(\frac{y'}{b/2}\right)_{\alpha_{LE}=72^\circ} = 0.45$ .

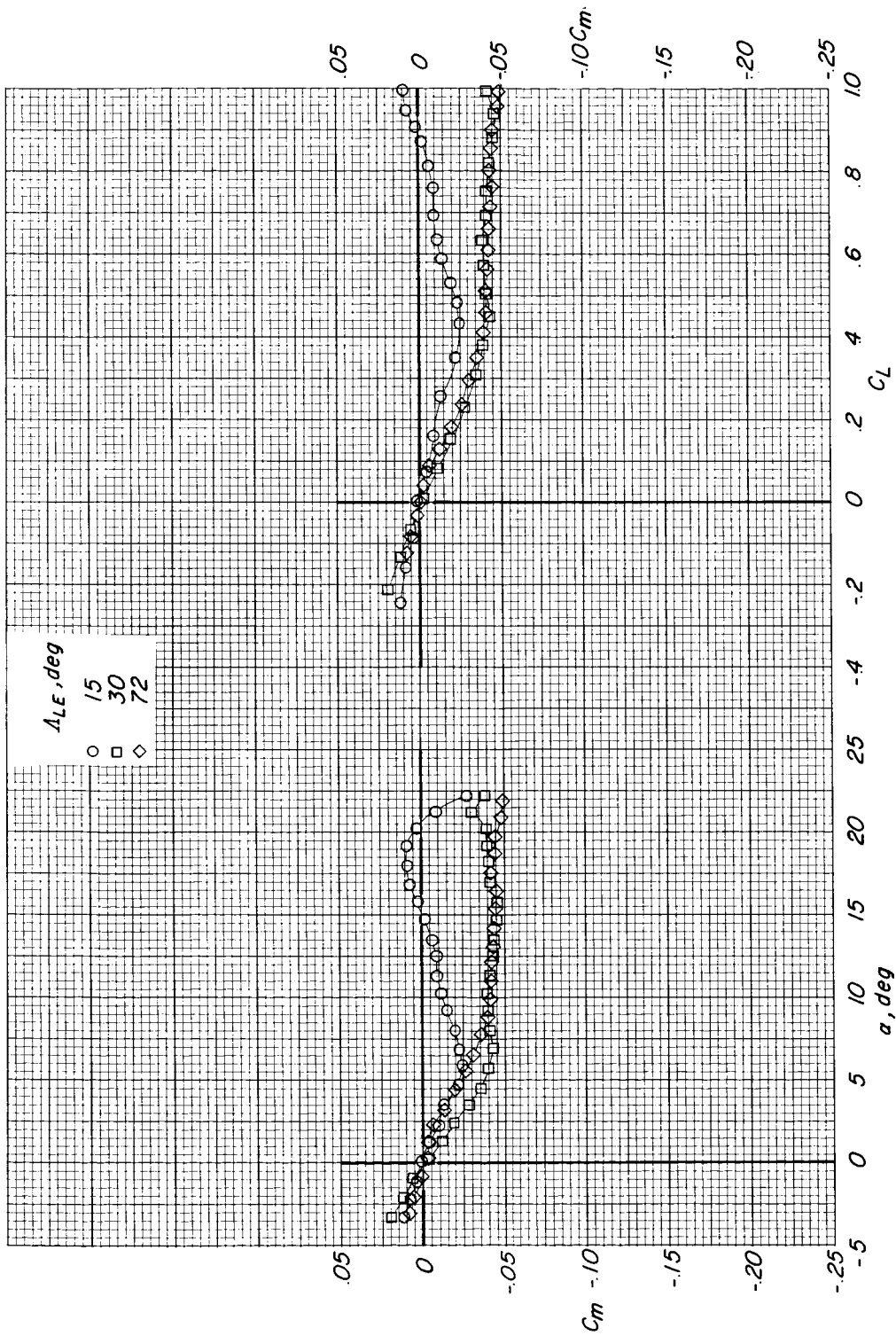


Figure 3.- Concluded.

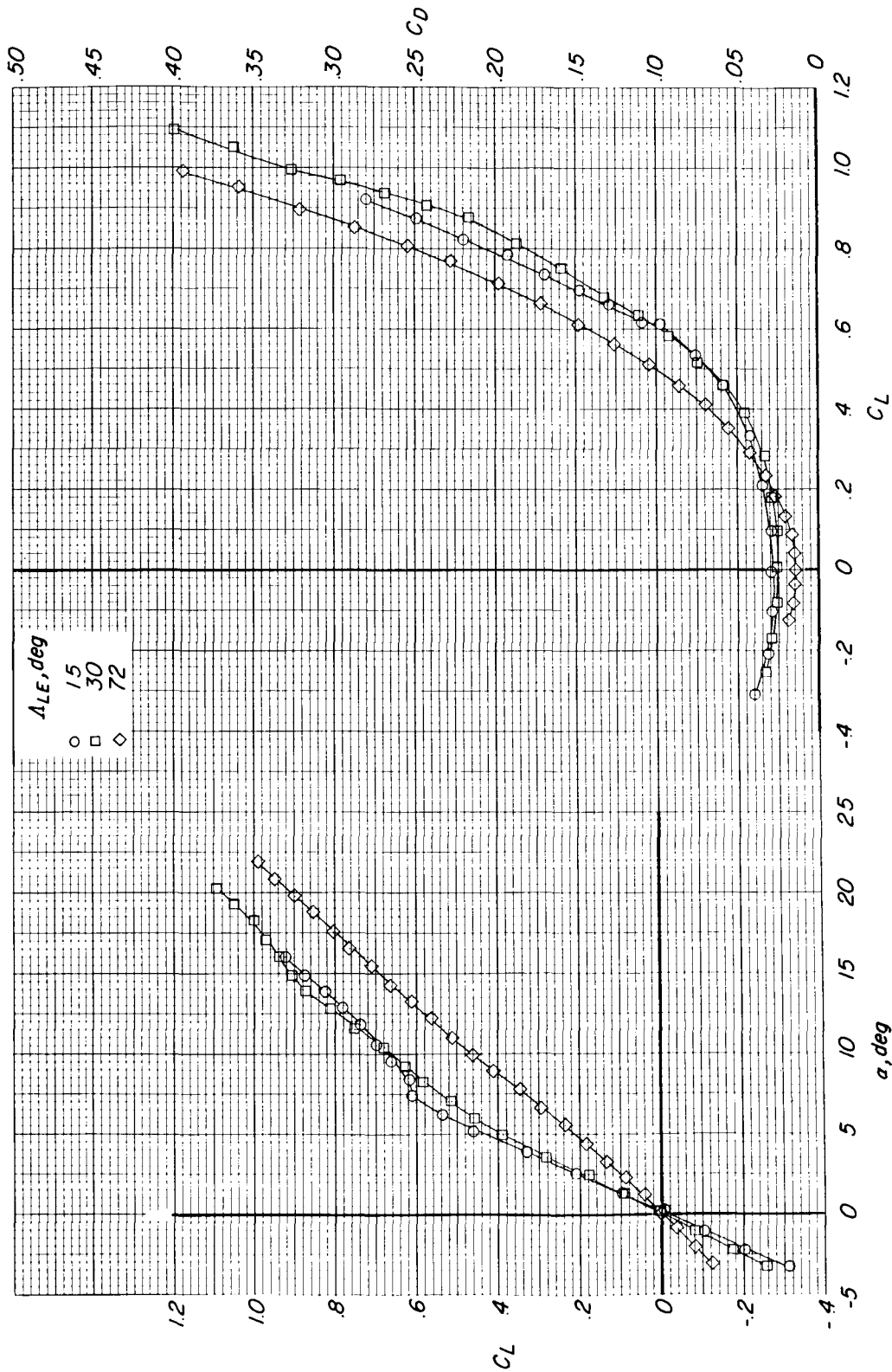


Figure 4.- Effect of wing leading-edge sweep angle on longitudinal aerodynamic characteristics of configuration with horizontal tails and engine packs off.  $\left(\frac{y'}{b/2}\right)_{A_{LE}=72^\circ} = 0.30$ .

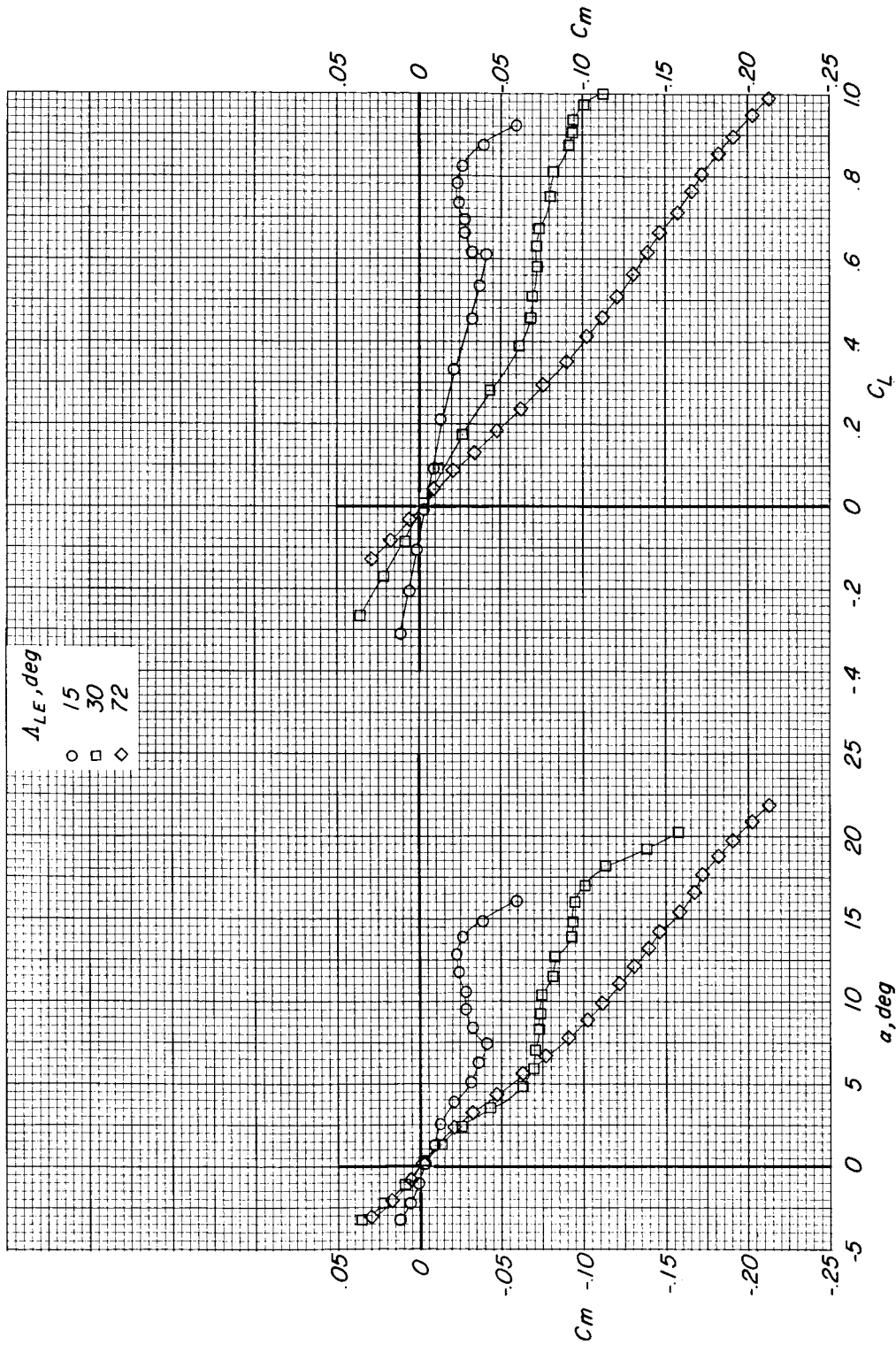


Figure 4.- Concluded.

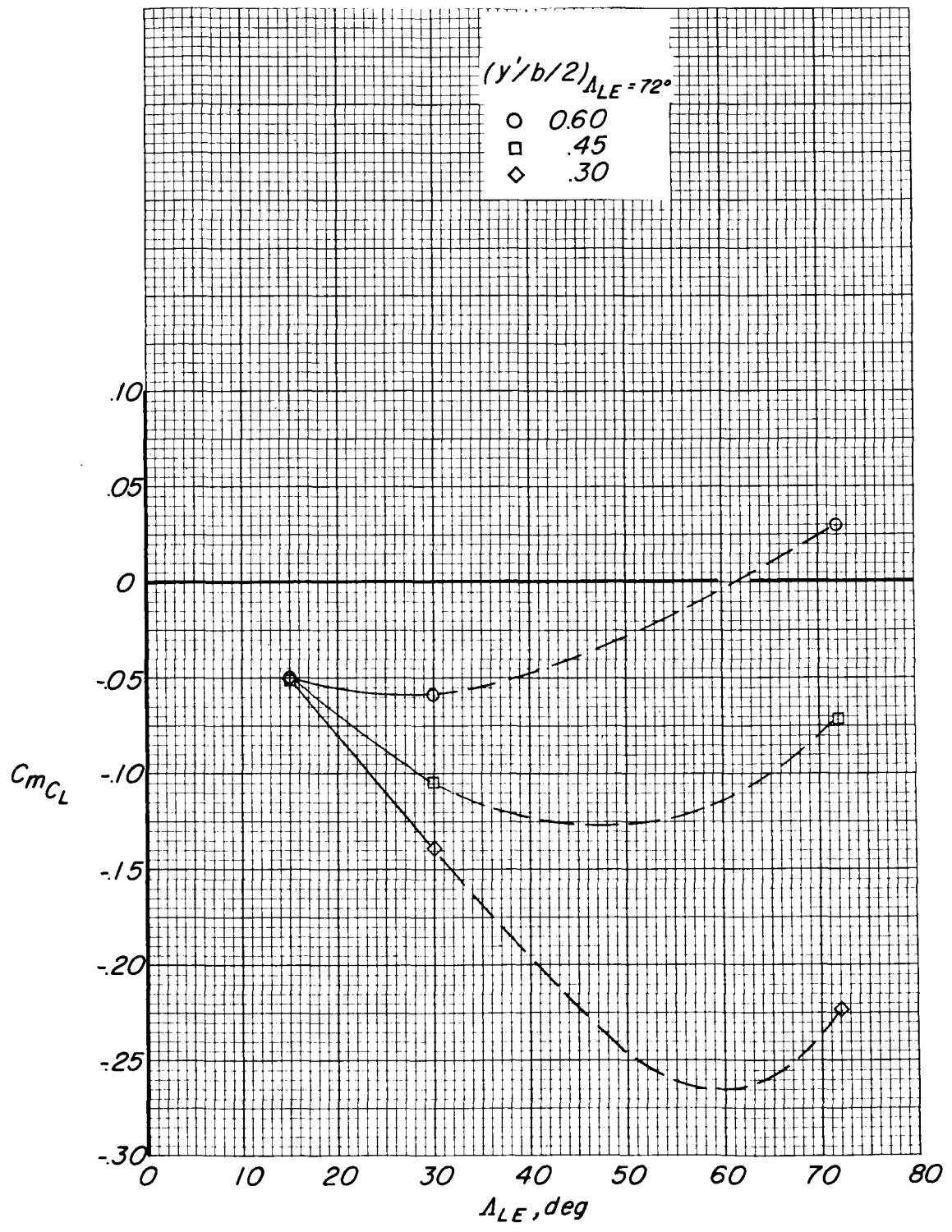


Figure 5.- Effect of pivot location on the variation of longitudinal stability parameter with wing leading-edge sweep angle for configuration with horizontal tails and engine packs off.

SECRET

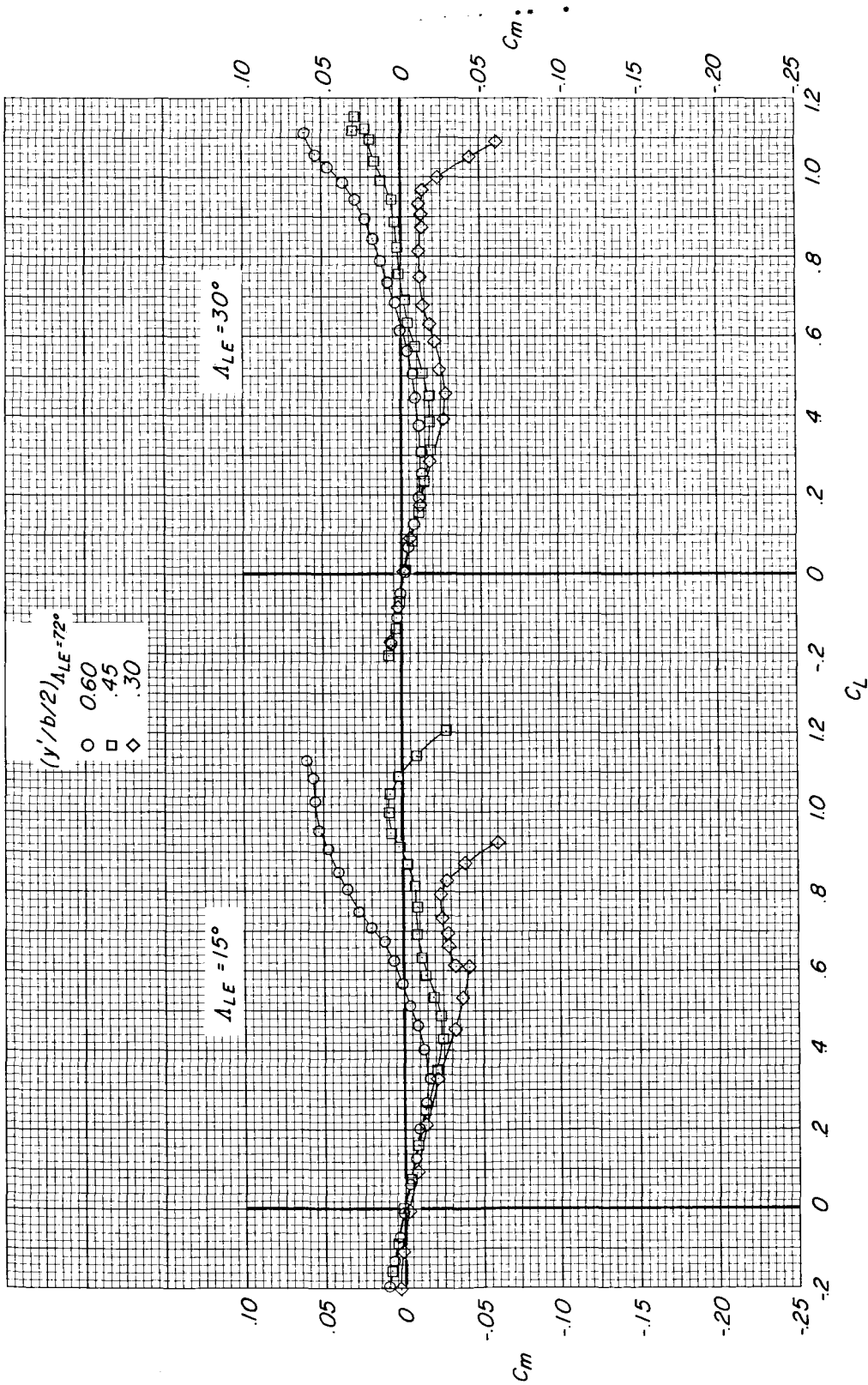


Figure 6.- Effect of pivot location on pitching-moment variation with lift coefficient for configuration with horizontal tails and engine packs off. (Transferred to same stability level through zero lift coefficient.)

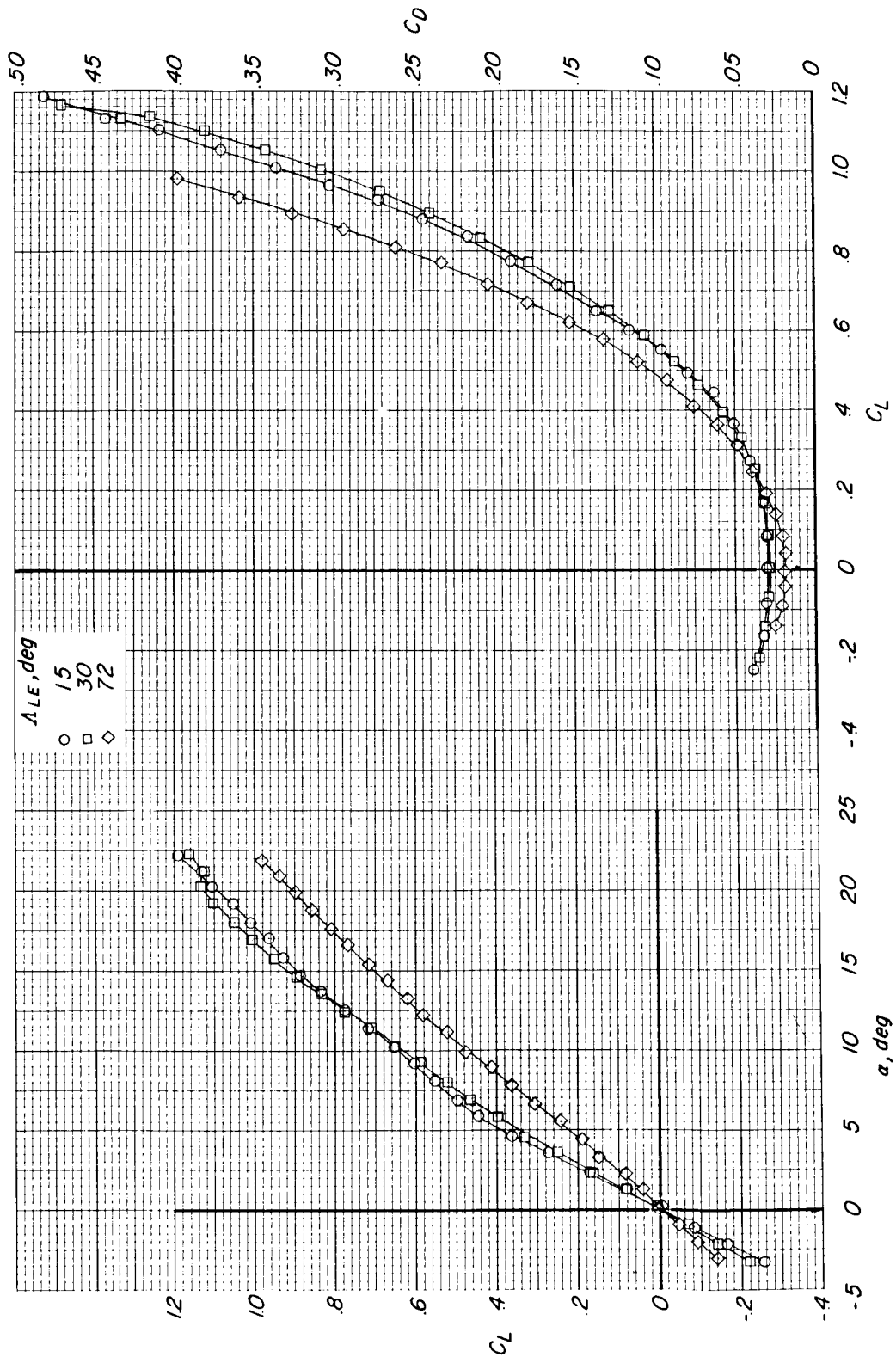


Figure 7.- Effect of wing leading-edge sweep angle on longitudinal aerodynamic characteristics of configuration with horizontal tails on (high location) and engine packs off.  $\left(\frac{y'}{b/2}\right)_{A_{LE}=72^\circ} = 0.45$ .

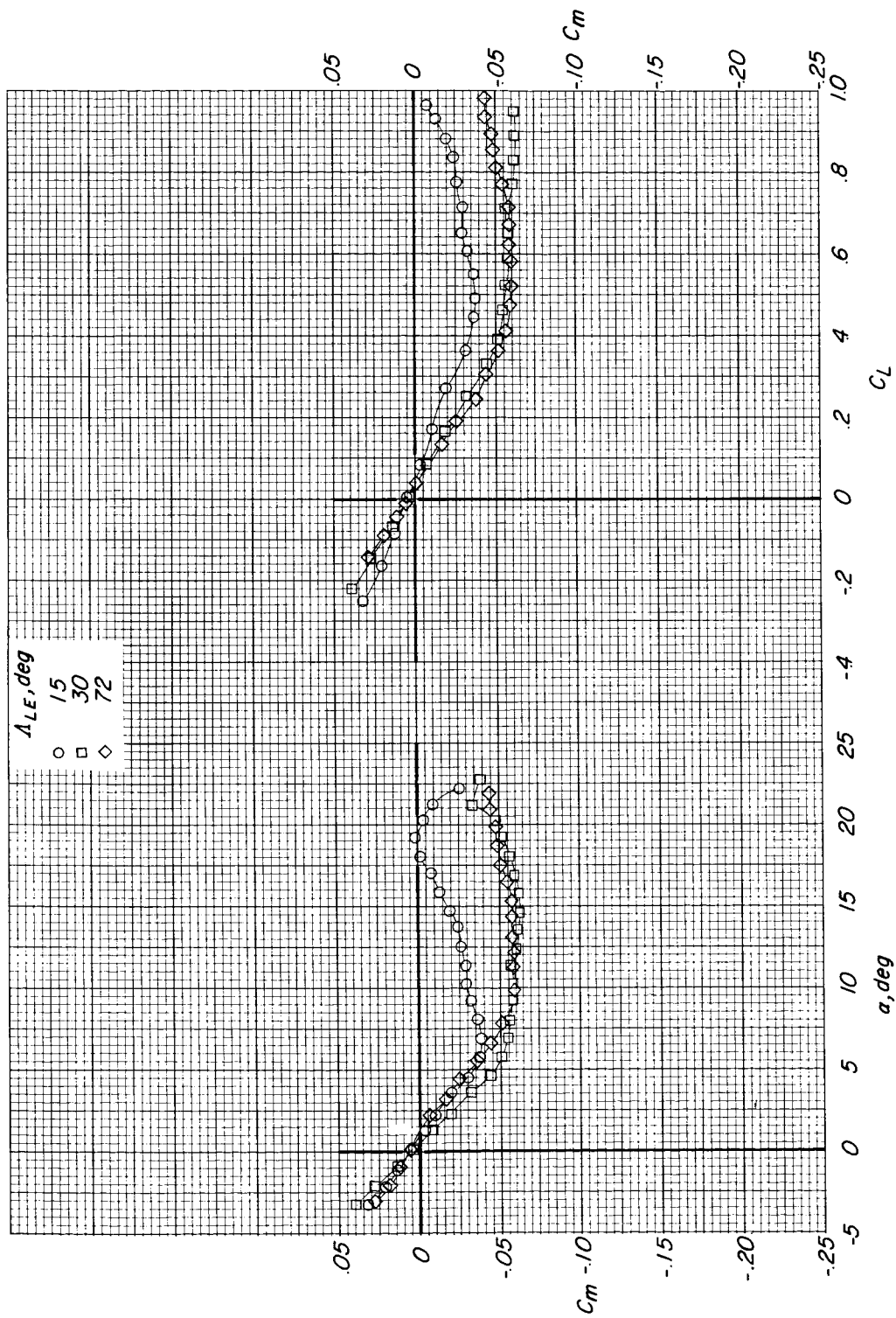


Figure 7.- Concluded.



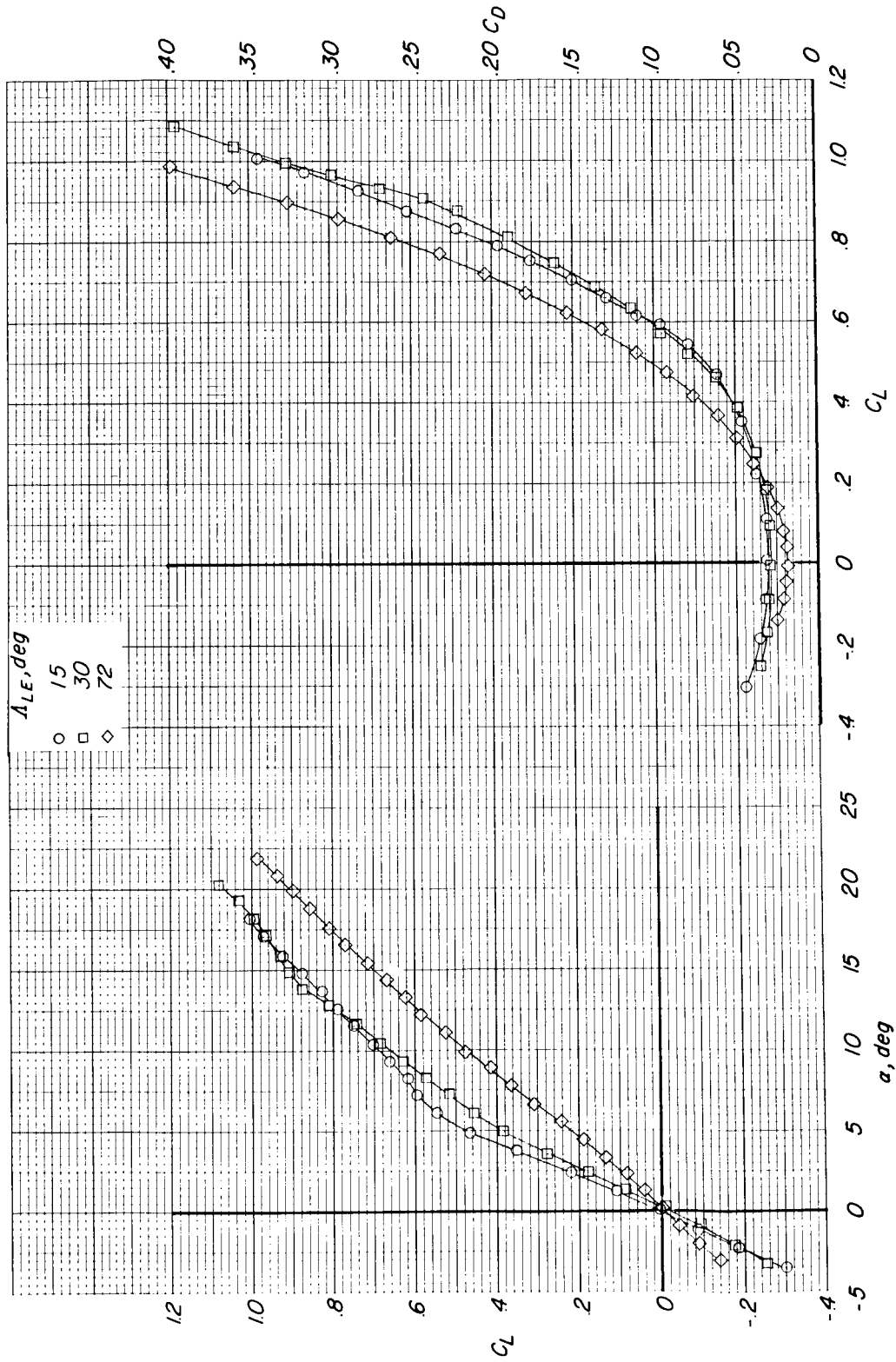


Figure 8.- Effect of wing leading-edge sweep angle on longitudinal aerodynamic characteristics of configuration with horizontal tails on (high location) and engine packs off.  $\left(\frac{y'}{b/2}\right)_{\Lambda_{LE}=72^\circ} = 0.30$ .

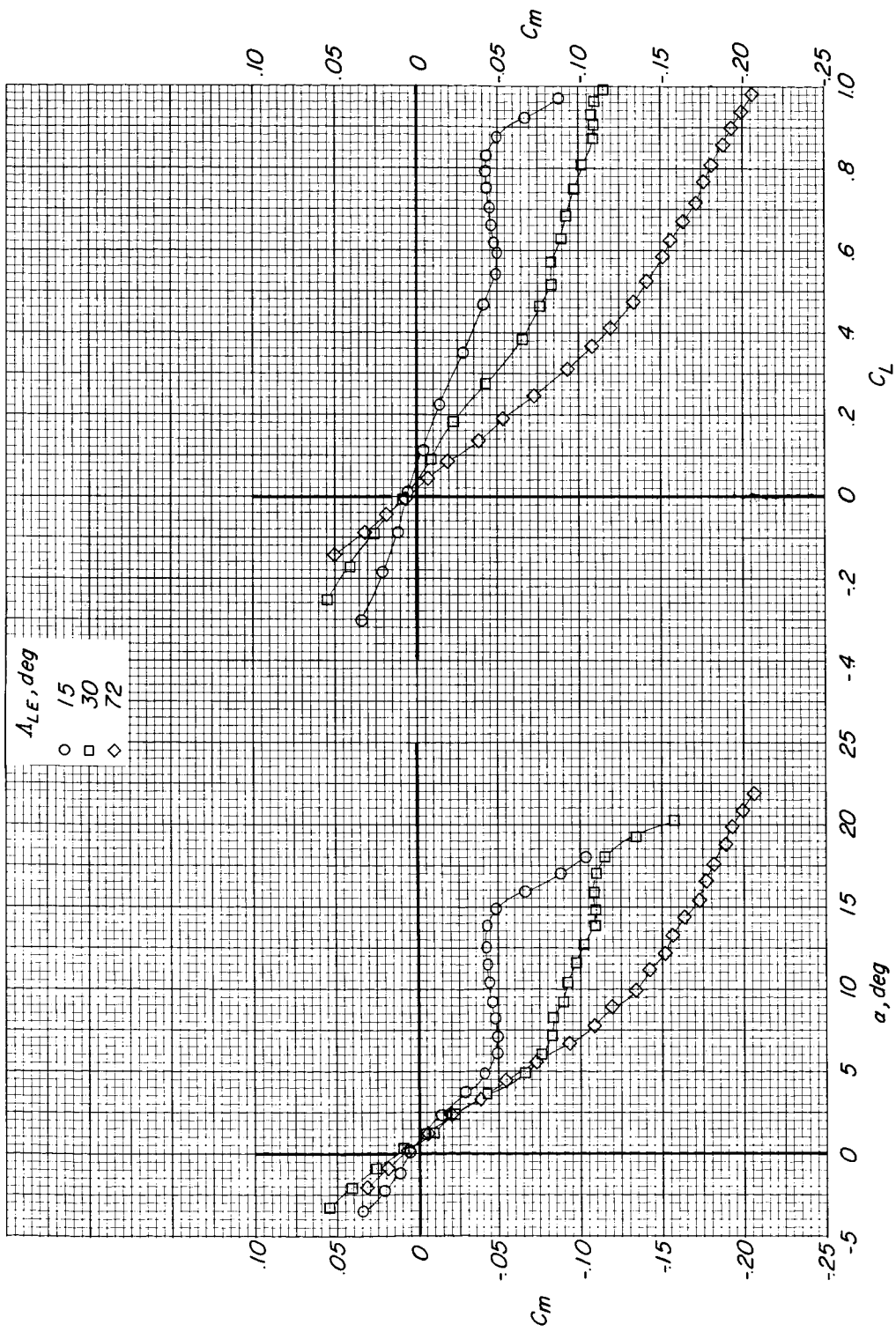


Figure 8.- Concluded.

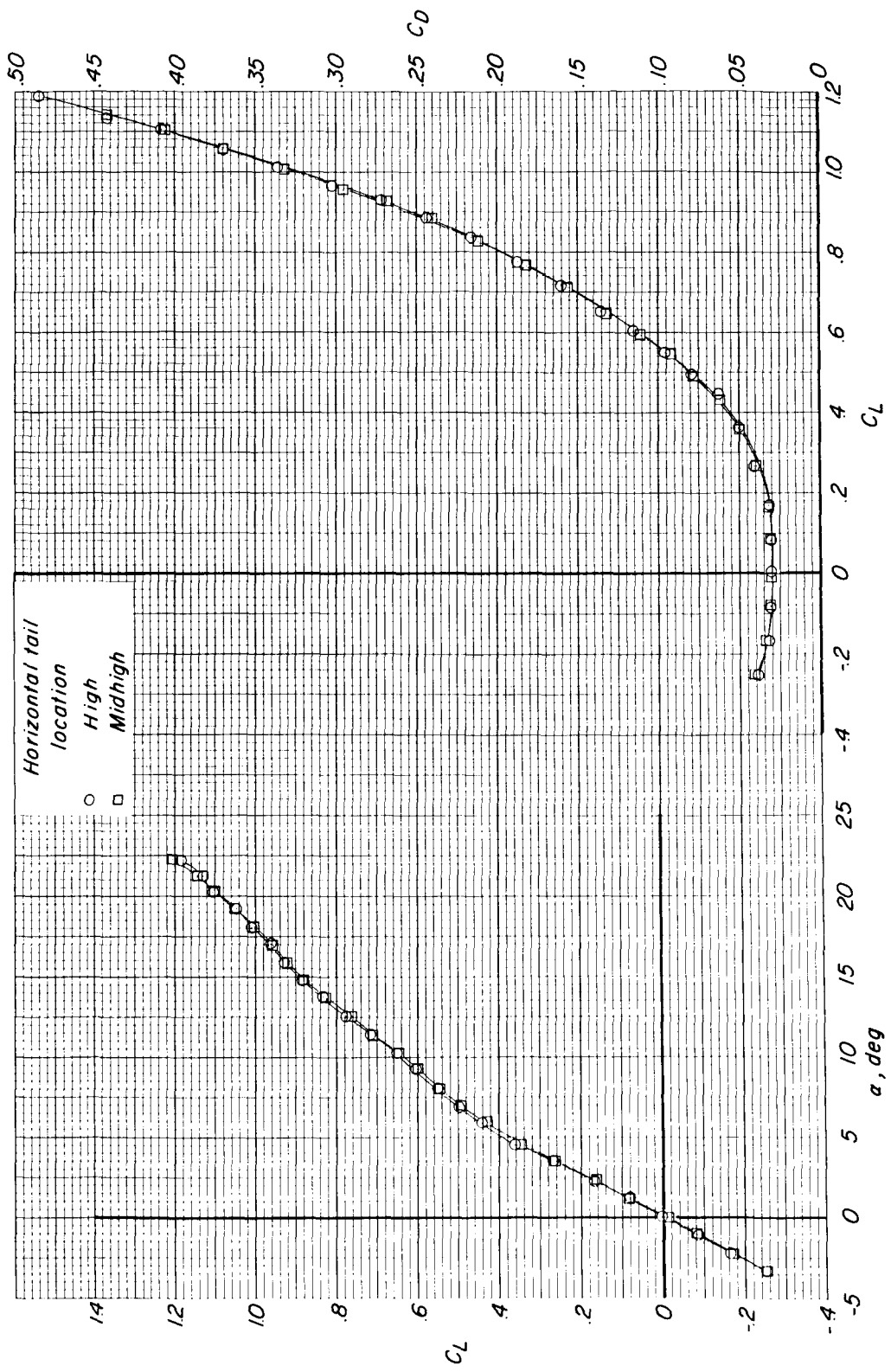


Figure 9.- Effect of location of horizontal tails on longitudinal aerodynamic characteristics of configuration with  $15^\circ$  of leading-edge sweep with engine packs off.  $\left(\frac{y'}{b/2}\right)_{\Lambda_{LE}=72^\circ} = 0.45$ .

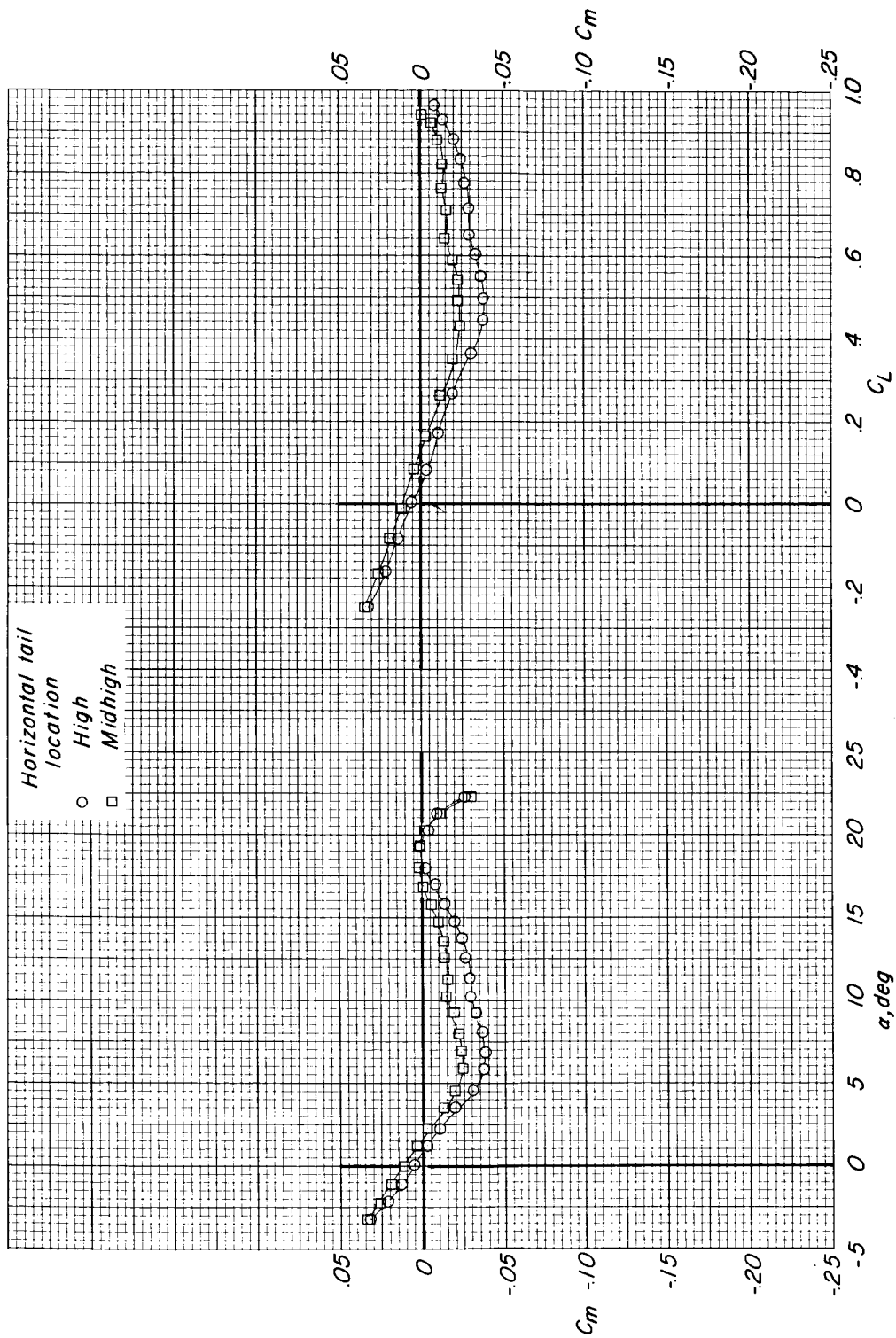


Figure 9.- Concluded.

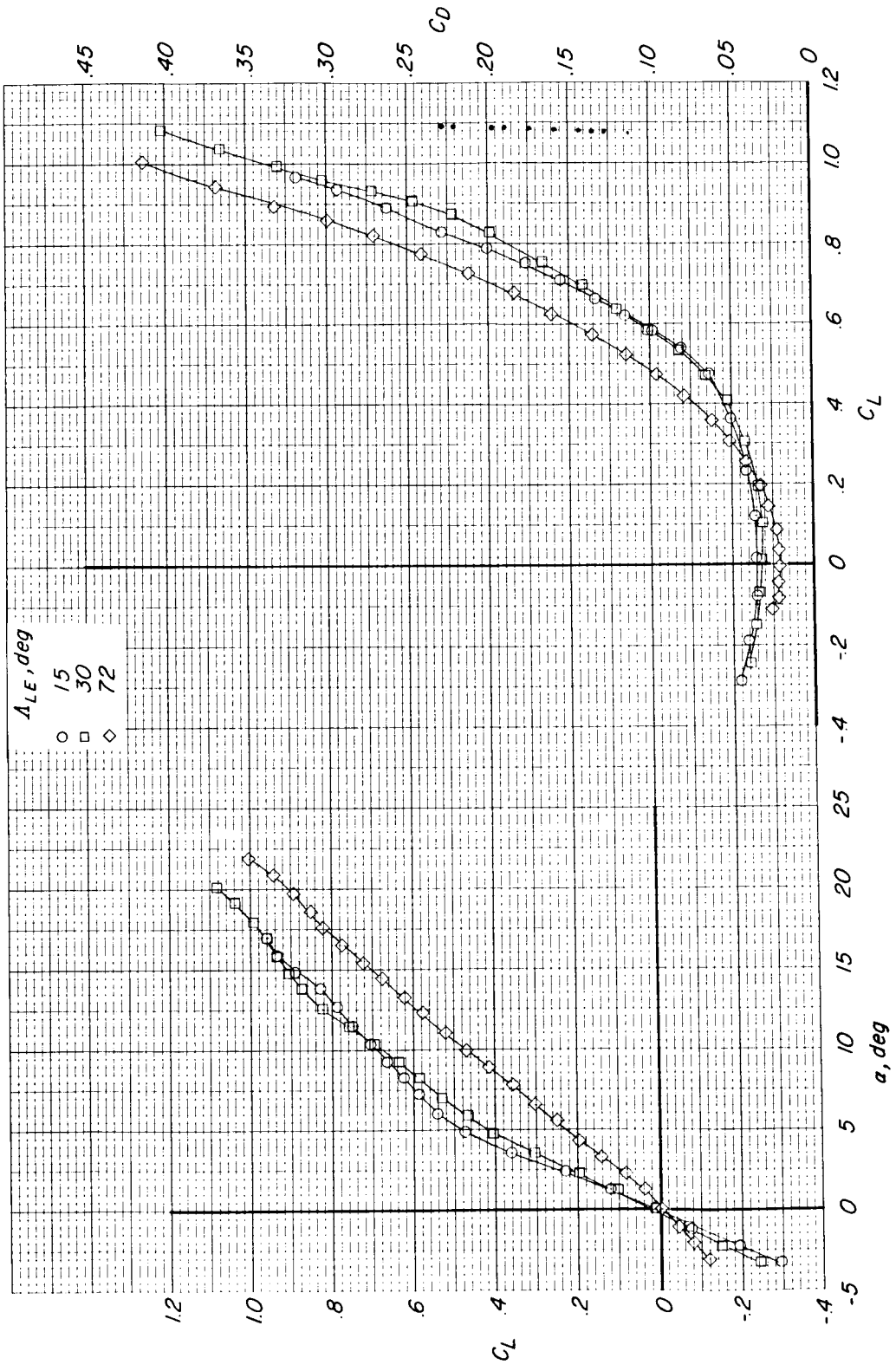


Figure 10.- Effect of wing leading-edge sweep angle on longitudinal aerodynamic characteristics of configuration with horizontal tails (high location) and engine packs on.  $\left(\frac{y'}{b/2}\right)_{A_{LE}=72^\circ} = 0.30$ .

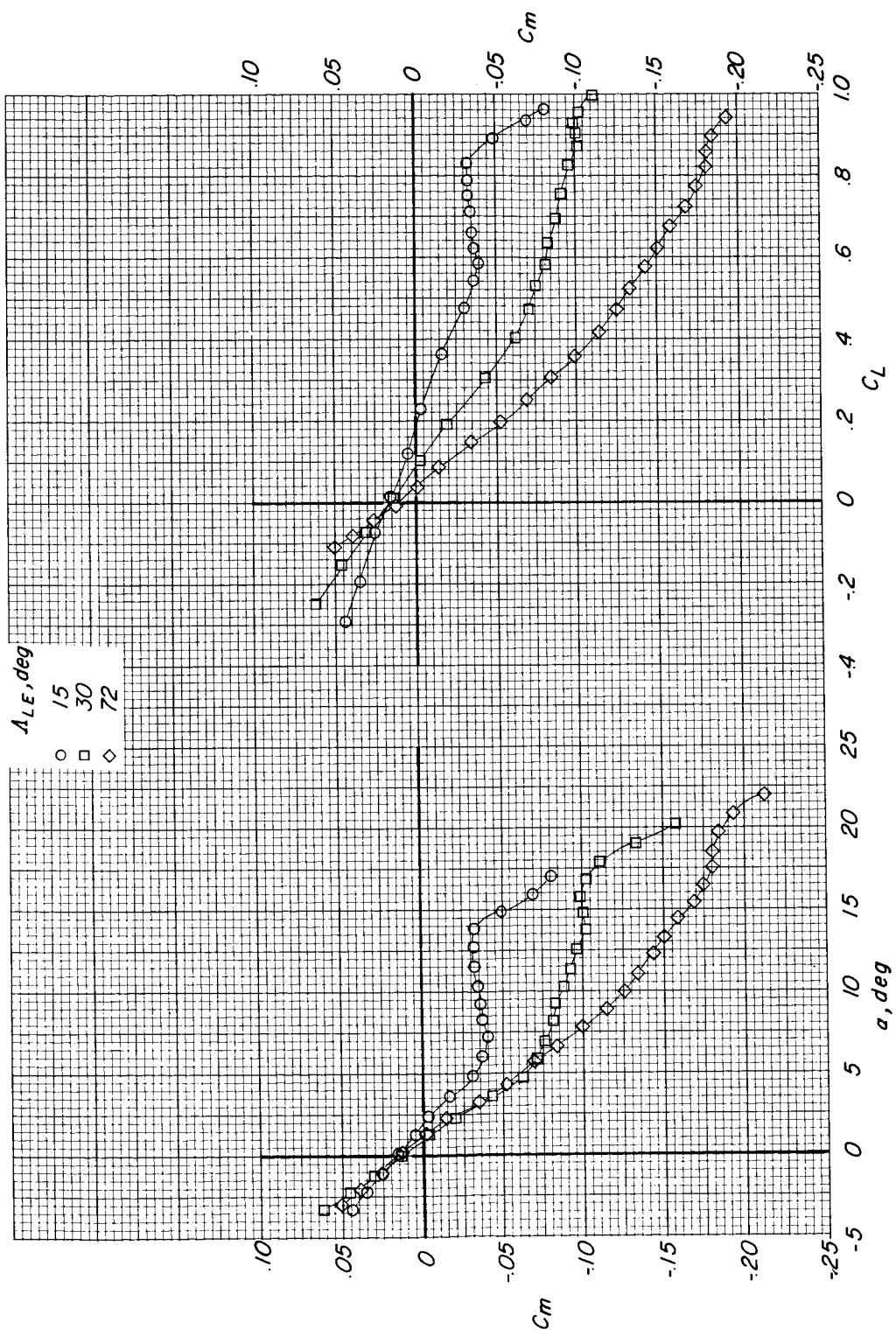


Figure 10.- Concluded.

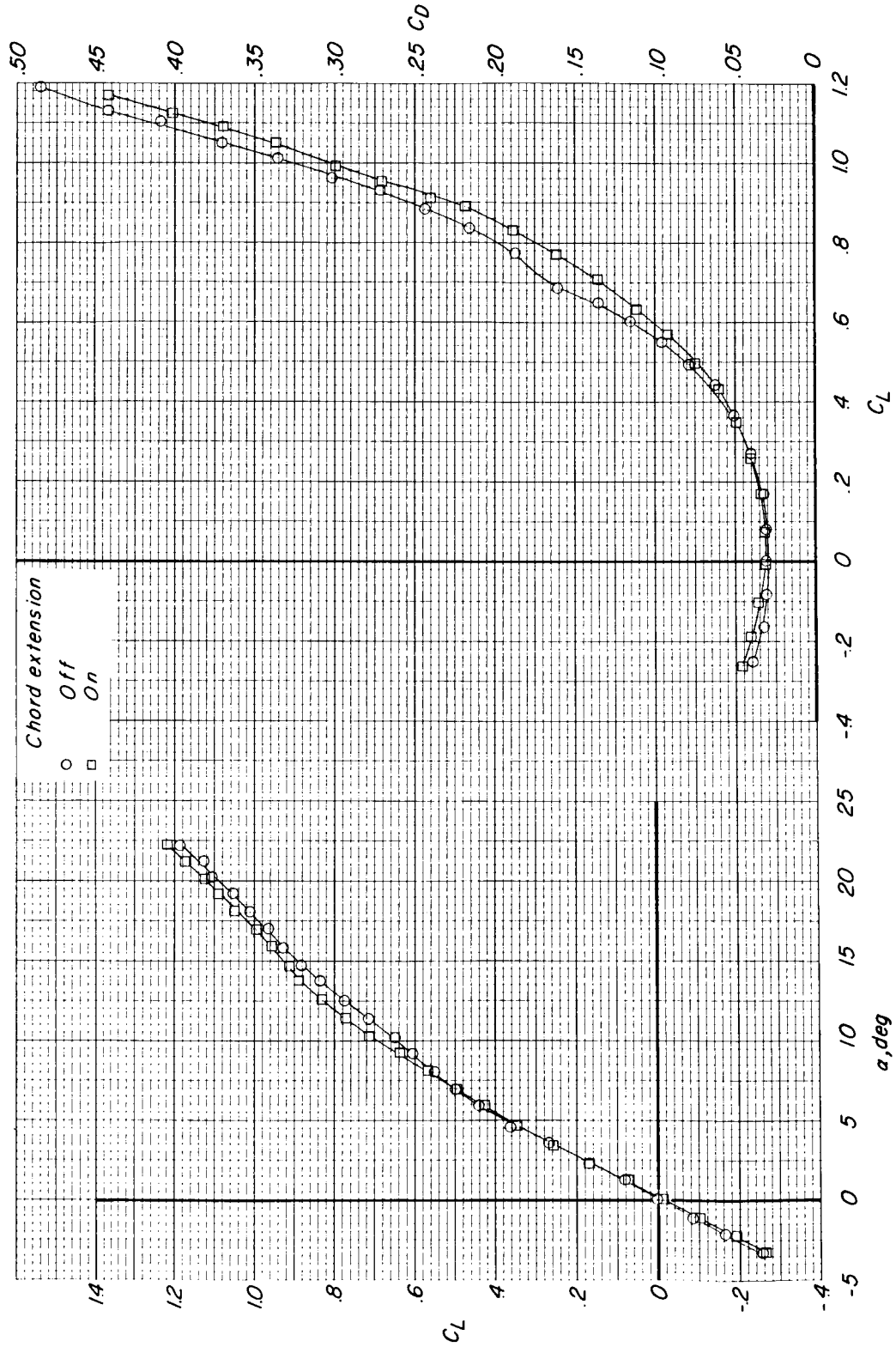


Figure 11.- Effect of chord extension on longitudinal aerodynamic characteristics of configuration with  $15^\circ$  of leading-edge sweep and horizontal tails on (high location) and engine packs off.  $\left(\frac{y'}{b/2}\right)_{A_{LE}} = 72^\circ = 0.45$ .

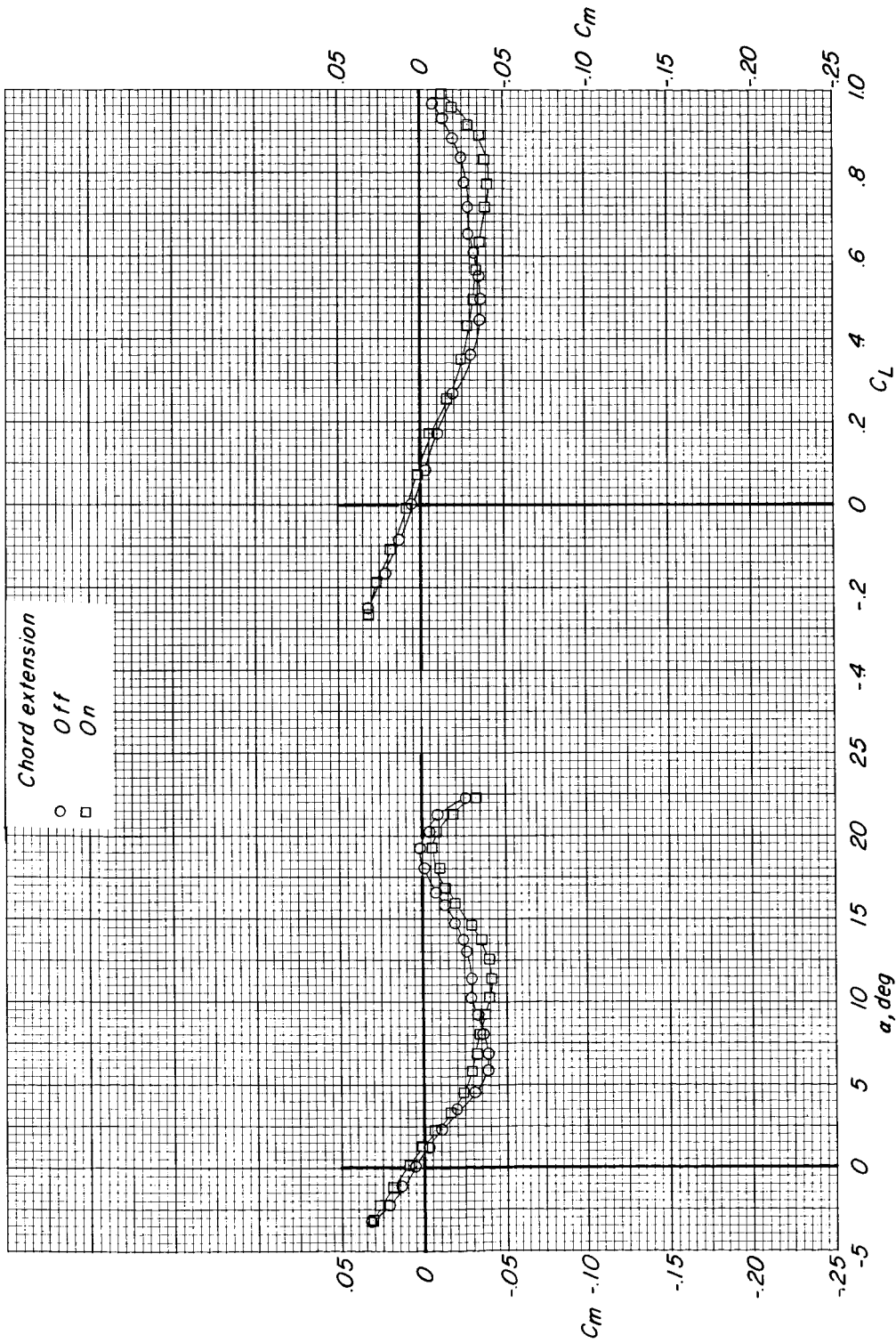


Figure 11.- Concluded.



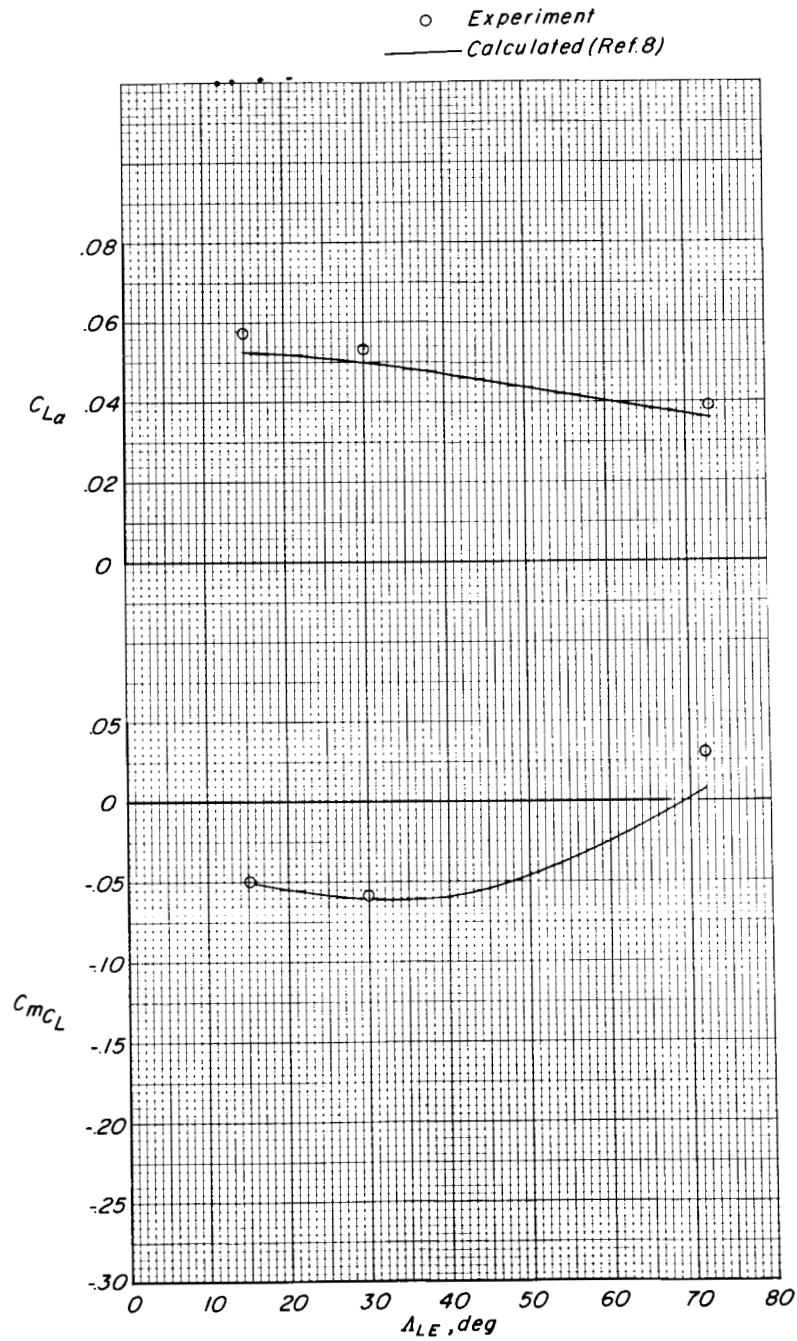


Figure 12.- Comparison of experimental and computed variation of lift-curve slope and longitudinal stability parameter with wing leading-edge sweep angle of configuration with horizontal tails

and engine packs off.  $\left(\frac{y'}{b/2}\right)_{\Delta_{LE}=72^\circ} = 0.60.$

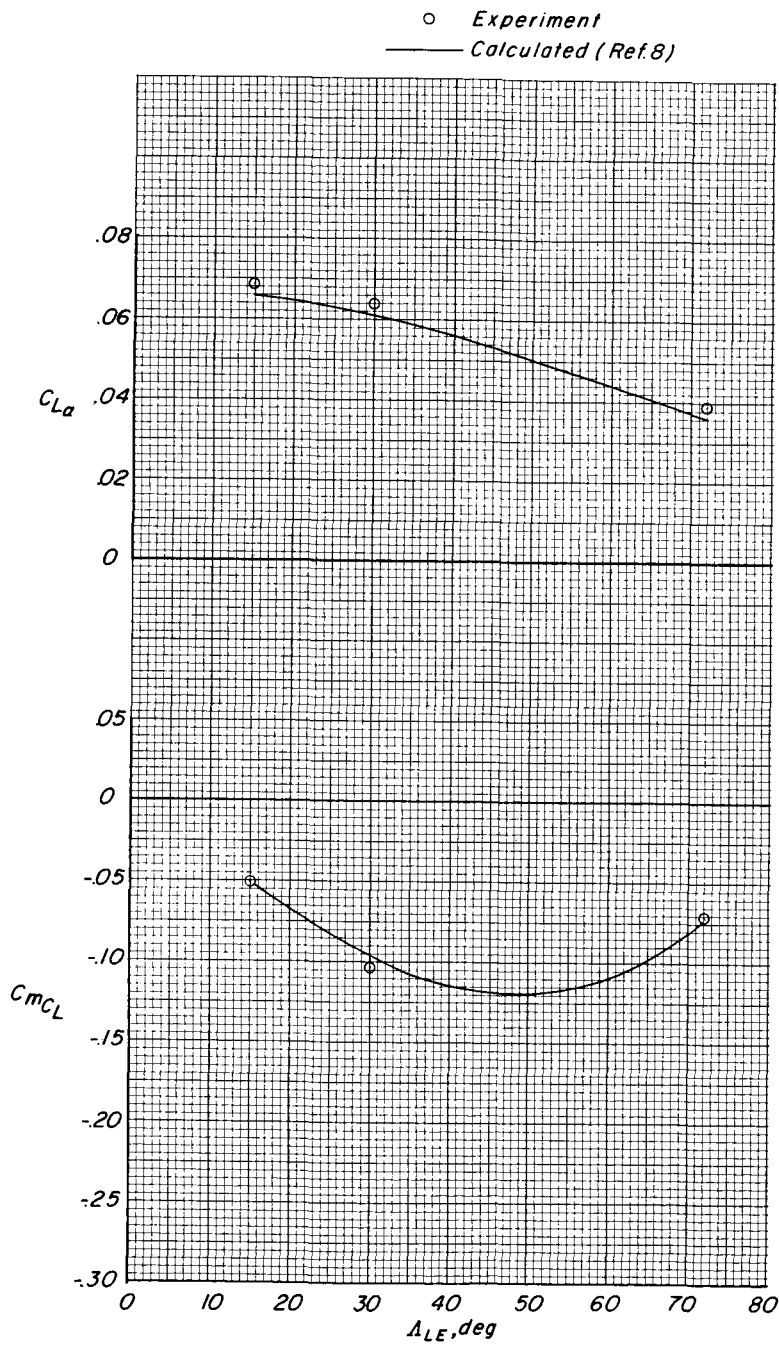


Figure 13.- Comparison of experimental and computed variation of lift-curve slope and longitudinal stability parameter with wing leading-edge sweep angle of configuration with horizontal tails

and engine packs off.  $\left(\frac{y'}{b/2}\right)_{\Delta_{LE}=72^\circ} = 0.45$ .

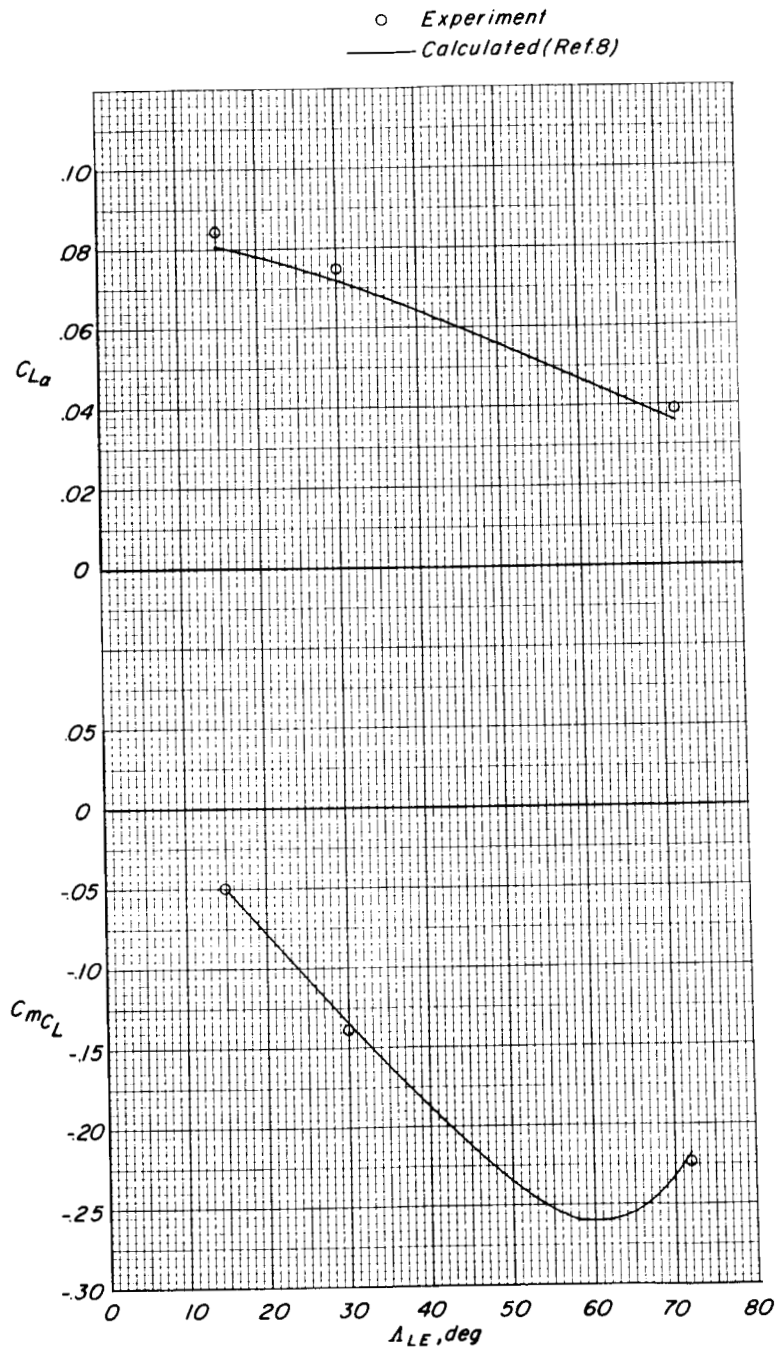


Figure 14.- Comparison of experimental and computed variation of lift-curve slope and longitudinal stability parameter with wing leading-edge sweep angle of configuration with horizontal tails and engine packs off.

$$\left(\frac{y'}{b/2}\right)_{\Delta_{LE}=72^\circ} = 0.30.$$

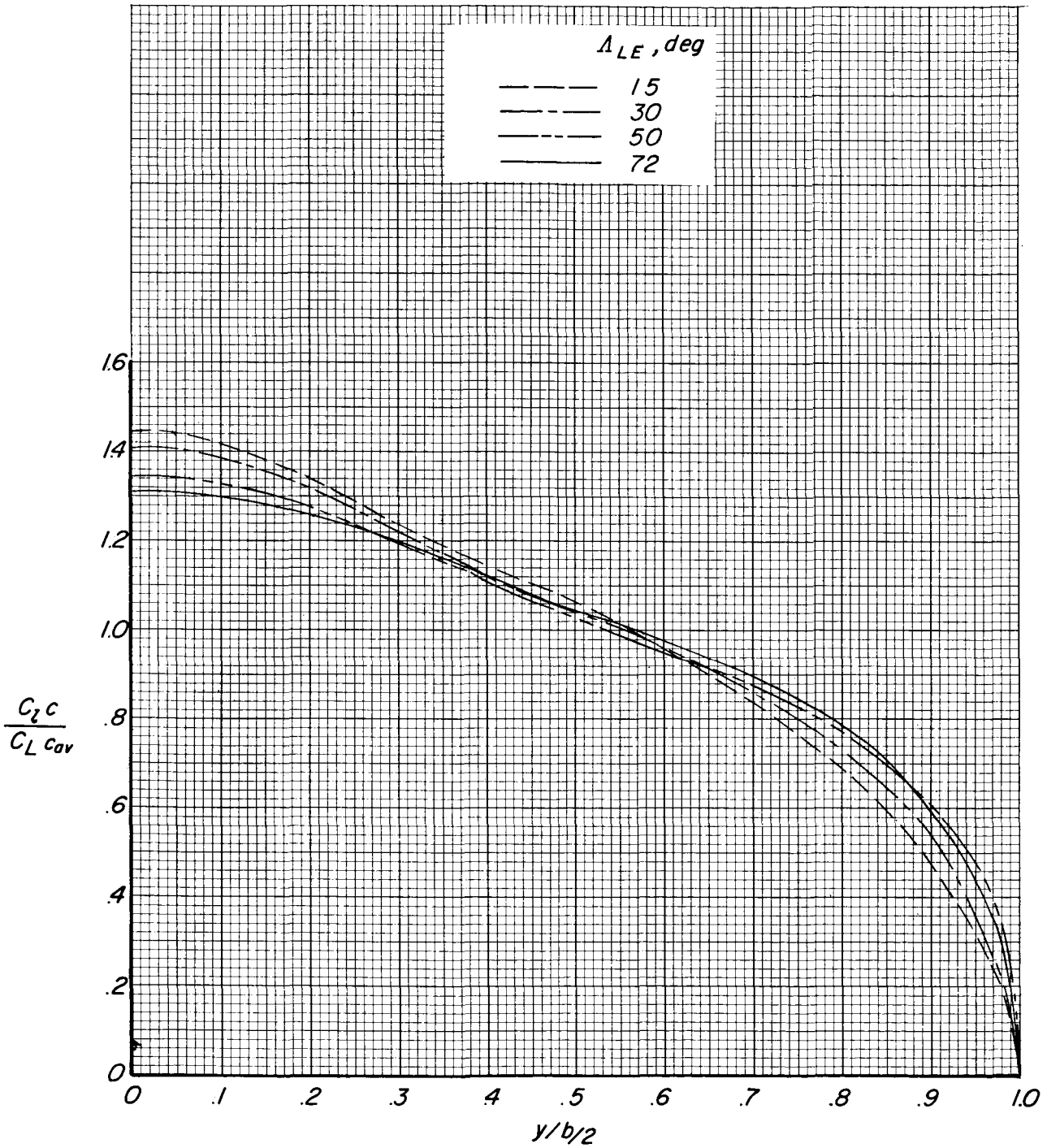


Figure 15.- Computed span-load distribution for wing alone, at various wing leading-edge sweep

angles.  $\left(\frac{y'}{b/2}\right)_{\Delta_{LE}=72^\circ} = 0.60.$

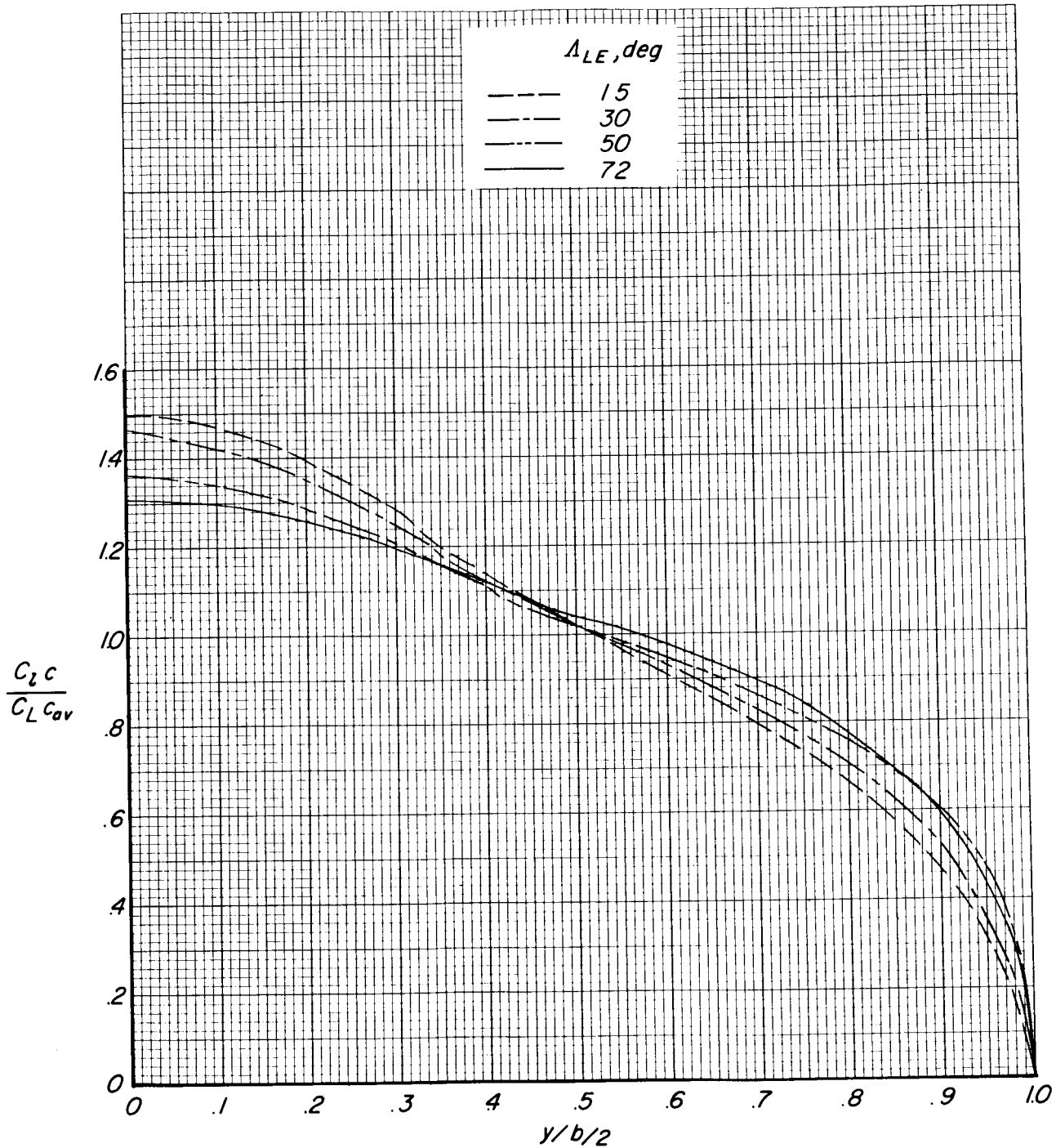


Figure 16.- Computed span-load distribution for wing alone, at various wing leading-edge sweep angles.  $\left(\frac{y'}{b/2}\right)_{\Lambda_{LE}=72^\circ} = 0.45$ .

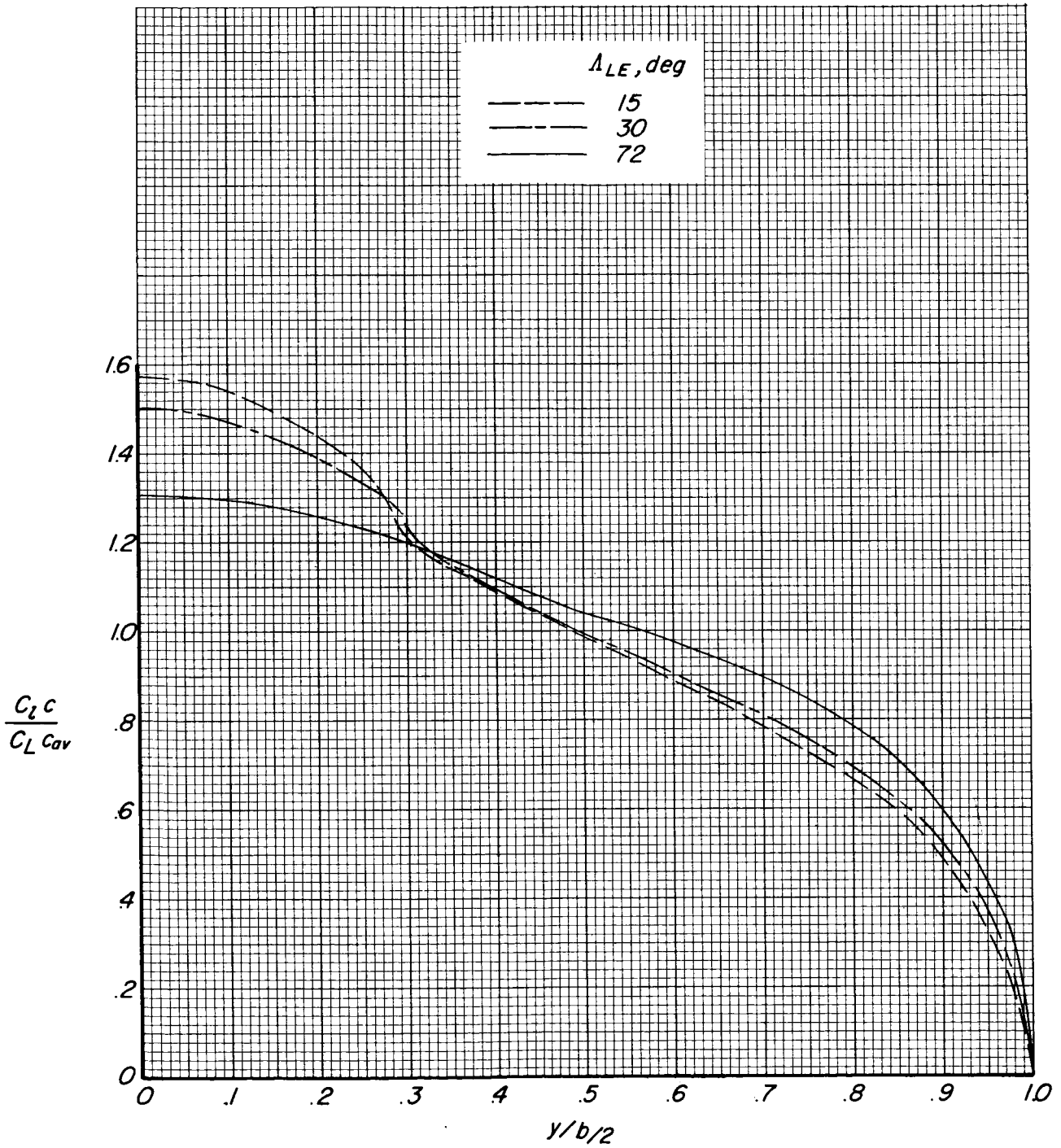


Figure 17.- Computed span-load distribution for wing alone, at various wing leading-edge sweep angles.  $\left(\frac{y'}{b/2}\right)_{\Lambda_{LE}=72^\circ} = 0.30$ .

*"The aeronautical and space activities of the United States shall be conducted so as to contribute . . . to the expansion of human knowledge of phenomena in the atmosphere and space. The Administration shall provide for the widest practicable and appropriate dissemination of information concerning its activities and the results thereof."*

—NATIONAL AERONAUTICS AND SPACE ACT OF 1958

## NASA SCIENTIFIC AND TECHNICAL PUBLICATIONS

**TECHNICAL REPORTS:** Scientific and technical information considered important, complete, and a lasting contribution to existing knowledge.

**TECHNICAL NOTES:** Information less broad in scope but nevertheless of importance as a contribution to existing knowledge.

**TECHNICAL MEMORANDUMS:** Information receiving limited distribution because of preliminary data, security classification, or other reasons.

**CONTRACTOR REPORTS:** Technical information generated in connection with a NASA contract or grant and released under NASA auspices.

**TECHNICAL TRANSLATIONS:** Information published in a foreign language considered to merit NASA distribution in English.

**TECHNICAL REPRINTS:** Information derived from NASA activities and initially published in the form of journal articles.

**SPECIAL PUBLICATIONS:** Information derived from or of value to NASA activities but not necessarily reporting the results of individual NASA-programmed scientific efforts. Publications include conference proceedings, monographs, data compilations, handbooks, sourcebooks, and special bibliographies.

*Details on the availability of these publications may be obtained from:*

SCIENTIFIC AND TECHNICAL INFORMATION DIVISION  
NATIONAL AERONAUTICS AND SPACE ADMINISTRATION

Washington, D.C. 20546